COMPTES RENDUS
(DOKLADY)
DE L'ACADÉMIE DES SCIENCES DE L'URSS

NOUVELLE SÉRIE

1943

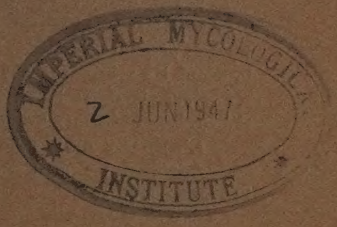

VOLUME XXXIX

№ 8

ÉDITION DE L'ACADÉMIE DES SCIENCES DE L'URSS
MOSCOU

AVIS AUX AUTEURS

Les «Comptes Rendus (Doklady) de l'Académie des Sciences de l'URSS» paraissent tous les dix jours. Neuf numéros composent un volume pourvu d'une table des matières. Il y a quatre volumes par année.

Les «Comptes Rendus de l'Académie des Sciences de l'URSS» en de courtes communications précisent l'essentiel des travaux en préparation. Ces articles, ne dépassant pas en règle générale quatre pages, sont donnés en anglais ou en français. Ils embrassent les sciences mathématiques, physiques, naturelles et appliquées, mettant au jour les résultats de recherches scientifiques en cours ou qui viennent d'être achevées, et représentant ainsi les plus récentes données de l'investigation scientifique.

L'auteur a droit à 25 exemplaires de son article.

Adressez les manuscrits à la Rédaction des «Comptes Rendus», Kazan, rue Baumann, 19.

20 Juin

COMPTES RENDUS

(DOKLADY)

DE L'ACADÉMIE DES SCIENCES DE L'URSS

COMITÉ DE RÉDACTION

A. Arbusov, de l'Académie, **A. Borissiak**, de l'Académie, **V. Chlopin**, de l'Académie, **A. Deborin**, de l'Académie, **A. Fersman**, de l'Académie, **A. Frumkin**, de l'Académie, **A. Kolmogoroff**, de l'Académie (vice rédacteur), **L. Orbéli**, de l'Académie (rédacteur en chef), **A. Richter**, de l'Académie, **S. Soboleff**, de l'Académie, **S. Wawilow**, de l'Académie (vice rédacteur)

NOUVELLE SÉRIE

11-me année

Paraissant tous les dix jours

1943

VOLUME XXXIX, № 8

TABLE DES MATIÈRES

MATHÉMATIQUES Pages

J. Geronimus. On Polynomials Orthogonal on the Circle, on Trigonometric Moment-Problem and on Allied Carathéodory and Schur Functions 291

ASTRONOMIE

B. Fessenkoff. Member of the Academy. On the Structural Features of the Solar Corona of Sept. 21, 1941 296

PHYSIQUE

W. W. Antonov-Romanovsky. Increase of Phosphorescence During Excitation . 299

PHYSIQUE DU GLOBE

N. N. Kalitin. Scattered Radiation of Cloudless Sky 303

HYDROMÉCANIQUE APPLIQUÉE

V. L. Posdunine. Member of the Academy. On the Working of Supercavitating Screw Propellers. 306

CHIMIE

B. A. Arbusov and E. V. Kuznetzov. On Addition Products of Dienes to Toluene . 311
N. N. Kurnakov. Studies on Solubility of Carbon in Silicomanganese 314

CHIMIE PHYSIQUE

N. S. Akulov. Member of the Academy of Sciences of the White Russian SSR. On the Diagram of Chemical Activity of Gases 317

N. N. Sirota. Two Types of *S*-curves in Isothermal Transformation of Supercooled Austenite 322

CHIMIE DU GLOBE

G. A. Maximovich. Hydrochemical Facies of Surface Geospheres 326

GÉOLOGIE

L. A. Vardanianz. Lower Jurassic Chain of Volcanoes in the Central Caucasus . . 329

Édition de l'Académie des Sciences de l'URSS
Moscou 1943

Comptes Rendus (Doklady) de l'Académie des Sciences de l'URSS
1943. Volume XXXIX, № 8

MATHEMATICS

ON POLYNOMIALS ORTHOGONAL ON THE CIRCLE, ON TRIGONOMETRIC MOMENT-PROBLEM AND ON ALLIED CARATHÉODORY AND SCHUR FUNCTIONS

By J. GERONIMUS

(Communicated by S. L. Sobolieff, Member of the Academy, 27. I. 1943)

I. Consider the polynomials $\{P_n(z)\}_0^\infty$ orthogonal on the unit-circle $z=e^{i\theta}$ with respect to the distribution $d\sigma(\theta)$

$$\frac{1}{2\pi}\int_0^{2\pi} P_n(e^{i\theta})\,\overline{P_m(e^{i\theta})}\,d\sigma(\theta)=\begin{cases}0, & n\neq m,\\ h_n>0, & n=m,\end{cases}\qquad P_n(z)=z^n+\ldots. \tag{1}$$

$\sigma(\theta)$ being a bounded non-decreasing function with infinitely many points of increase in $<0,\ 2\pi>$; we have the relations (1):

$$P_{n+1}(z)=zP_n(z)-\bar{a}_nP_n^*(z),\quad P_n^*(z)=z^n\,\overline{P}_n\left(\frac{1}{z}\right);$$

$$(-1)^n a_n=|c_{i-k+1}|_0^n:|c_{i-k}|_0^n, \tag{2'}$$

$$h_n=|c_{i-k}|_0^n:|c_{i-k}|_0^{n-1}=h_0\prod_{k=0}^{n-1}(1-|a_k|^2), \tag{2''}$$

$$c_n=\frac{1}{2\pi}\int_0^{2\pi}e^{-in\theta}d\sigma(\theta)\quad c_{-n}=\bar{c}_n,\quad (n=0,\ 1,\ 2,\ \ldots.); \tag{3}$$

the functions

$$F(z)=\frac{1}{2\pi c_0}\int_0^{2\pi}\frac{e^{i\theta}+z}{e^{i\theta}-z}\,d\sigma(\theta),\ f(z)=\frac{1}{z}\,\frac{F(z)-1}{F(z)+1},\quad |z|<1 \tag{4}$$

will be called C-, resp. S-functions; in the domain $|z|<1$ they are regular and satisfy the inequalities

$$RF(z)>0,\quad |f(z)|<1. \tag{5}$$

Theorem I. *If* $\{|a_i|\}_0^{n-1}<1$, *then the points corresponding to the values assumed by a C-function* $F(z)$ *at the point* z *of the domain* $|z|<1$ *are located inside the circle* $K_n(z)$ *with centre* $C_n(z)$ *and radius* $r_n(z)$

$$C_n(z)=\frac{\overline{P_n^*(z)}\,Q_n^*(z)+|z|^2\overline{P_n(z)}\,Q_n(z)}{|P_n^*(z)|^2-|zP_n(z)|^2},\qquad r_n(z)=\frac{2h_n|z|^{n+1}}{c_0\{|P_n^*(z)|^2-|zP_n(z)|^2\}}; \tag{6}$$

the polynomials $\Omega_n(z)$ are connected by the relation

$$\Omega_{n+1}(z)=z\Omega_n(z)+\bar{a}_n\Omega_n^*(z),\quad (n=0,1,2,\ldots),\quad \Omega_0=1, \tag{7}$$

analogous to (2'); for all $|a_n|<1$ the point w_n is located inside $K_n(z)$ and the point w_n' outside it, where

$$w_n=\frac{\Omega_{n+1}^*(z)}{P_{n+1}^*(z)}=\frac{\Omega_n^*(z)+za_n\Omega_n(z)}{P_n^*(z)-za_nP_n(z)},\quad w_n'=-\frac{\Omega_{n+1}(z)}{P_{n+1}(z)}=-\frac{z\Omega_n(z)+\bar{a}_n\Omega_n^*(z)}{zP_n(z)-\bar{a}_nP_n^*(z)}. \tag{8}$$

An immediate consequence of Theorem I is that the conditions $\{|a_\nu|\}_0^\infty<1$ are necessary and sufficient for the solvability of the trigonometric moment-problem (3) and consequently for the construction of C- and S-functions (4); if $\{|a_\nu|\}_0^{n-1}<1$, $|a_n|=1$, these functions become

$$F(z)=-\frac{\Omega_{n+1}(z)}{P_{n+1}(z)},\quad f(z)=\frac{1}{z}\,\frac{\Omega_{n+1}(z)+P_{n+1}(z)}{\Omega_{n+1}(z)-P_{n+1}(z)}=\frac{p_n(z)}{p_n^*(z)}, \tag{9}$$

where the roots of the polynomials $P_{n+1}(z)$ and $\Omega_{n+1}(z)$ are distinct, lie on the circle $|z|=1$ and separate each other; $p_n(z)$ is a polynomial of degree n with all roots in the domain $|z|<1$; in this case of degeneration the points of increase of the function $\sigma(\theta)$ are $\{\theta_k\}_1^{n+1}$, where $\{P_{n+1}(e^{i\theta_k})\}_1^{n+1}=0$.

Theorem II. *If $0<\{|a_\nu|\}_0^\infty<1$, then the C-function $F(z)$ and the S-function $f(z)$ have the following continued-fraction expansions:*

$$F(z)=1+\cfrac{2a_0z}{1-a_0z}-\cfrac{\frac{a_1}{a_0}z(1-|a_0|^2)}{1+\frac{a_1}{a_0}z}-\cfrac{\frac{a_2}{a_1}z(1-|a_1|^2)}{1+\frac{a_2}{a_1}z}-\ldots, \tag{10}$$

$$f(z)=\cfrac{a_0}{1}-\cfrac{\frac{a_1}{a_0}z(1-|a_0|^2)}{1+\frac{a_1}{a_0}z}-\cfrac{\frac{a_2}{a_1}z(1-|a_1|^2)}{1+\frac{a_2}{a_1}z}-\ldots, \tag{10'}$$

converging uniformly in the closed domain $|z|\leqslant r<1$; their convergents of order n give the approximation of order not lower than $O(r^n)$; conversely, under condition $0<\{|a_\nu|\}_0^\infty<1$ the continued fractions (10) and (10') converge uniformly in the said domain and represent a C-, resp. a S-function.

Theorem III. *The functions $\{f_\nu(z)\}_0^\infty$ constructed by means of Schur's algorithm* [3]

$$f_{\nu+1}(z)=\frac{1}{z}\,\frac{f_\nu(z)-f_\nu(0)}{1-\overline{f_\nu(0)}\,f_\nu(z)},\quad f_0(z)=f(z), \tag{11}$$

are given by the formulae

$$f_\nu(z)=\frac{1}{z}\,\frac{zf_0(z)[P_\nu^*(z)+\Omega_\nu^*(z)]+P_\nu^*(z)-\Omega_\nu^*(z)}{zf_0(z)[P_\nu(z)-\Omega_\nu(z)]+P_\nu(z)+\Omega_\nu(z)}; \tag{12}$$

*Schur's parameters $\{f_\nu(0)\}_0^\infty$ coincide with our parameters $\{a_\nu\}_0^\infty$; the functions $\{f_\nu(z)\}_0^\infty$ are S-functions if and only if**

$$\{|f_\nu(0)|\}_0^\infty=\{|a_\nu|\}_0^\infty<1; \tag{13}$$

in the same way we have for C-functions

$$F_{\nu+1}(z)=\frac{z[F_\nu(z)+1]\left[1-\frac{1}{2}F_\nu'(0)\right]+[F_\nu(z)-1]\left[1-\frac{1}{2}\overline{F_\nu'(0)}\right]}{z[F_\nu(z)+1]\left[1+\frac{1}{2}F_\nu'(0)\right]-[F_\nu(z)-1]\left[1+\frac{1}{2}\overline{F_\nu'(0)}\right]},$$

* We exclude the case of degeneration.

$$F_0(z)=F(z), \tag{14}$$

$$F_\nu(z)=\frac{F_0(z)\,[P_\nu(z)+P_\nu^*(z)]+Q_\nu(z)-Q_\nu^*(z)}{F_0(z)\,[P_\nu(z)-P_\nu^*(z)]+Q_\nu(z)+Q_\nu^*(z)}, \qquad a_\nu=\frac{1}{2}F_\nu'(0); \tag{15}$$

if $0<\{|a_\nu|\}_0^\infty<1$, *then the functions* $\{f_\nu(z)\}_0^\infty$ *and* $\{F_\nu(z)\}_0^\infty$ *have the continued-fraction expansions**

$$f_\nu(z)=\frac{a_\nu}{|1}-\frac{\dfrac{a_{\nu+1}}{a_\nu}z(1-|a_\nu|^2)}{\left|1+\dfrac{a_{\nu+1}}{a_\nu}z\right.}-\frac{\dfrac{a_{\nu+2}}{a_{\nu+1}}z(1-|a_{\nu+1}|^2)}{\left|1+\dfrac{a_{\nu+2}}{a_{\nu+1}}z\right.}-\ldots, \tag{16}$$

$$F_\nu(z)=1+\frac{2a_\nu z}{|1-a_\nu z}-\frac{\dfrac{a_{\nu+1}}{a_\nu}z(1-|a_\nu|^2)}{\left|1+\dfrac{a_{\nu+1}}{a_\nu}z\right.}-\frac{\dfrac{a_{\nu+2}}{a_{\nu+1}}z(1-|a_{\nu+1}|^2)}{\left|1+\dfrac{a_{\nu+2}}{a_{\nu+1}}z\right.}-\ldots, \tag{16'}$$

converging uniformly in the closed domain $|z|\leqslant r<1$.

II. The knowledge of the parameters $\{a_n\}_0^\infty$ enables us to draw some conclusions concerning the set E of the points of increase of the function $\sigma(\vartheta)$; let

$$\left.\begin{aligned}p_{\nu+1}(z)&=zp_\nu(z)-\bar{a}_\nu p_\nu^*(z)\\ \omega_{\nu+1}(z)&=z\omega_\nu(z)+\bar{a}_\nu\omega_\nu^*(z)\end{aligned}\right\}\ (\nu=0,1,2,\ldots,k-1),\ p_0=1,\quad \omega_0=1; \tag{17}$$

$$\Phi^2(z)=\{p_k(z)+\omega_k(z)+p_k^*(z)+\omega_k^*(z)\}^2-16z^k\prod_{i=0}^{k-1}(1-|a_i'|^2), \tag{17'}$$

$$E_0=<\vartheta_1,\ \vartheta_2>+<\vartheta_3,\ \vartheta_4>+\ldots+<\vartheta_{2m-1},\ \vartheta_{2m}>,\quad (m\leqslant k), \tag{18}$$

where $\{z_r=e^{i\vartheta_r}\}_1^{2m}$ are the branch-points of the algebraic function $\varphi(z)$**.

Theorem IV. *If the parameters possess the property*

$$\lim_{n\to\infty}a_{kn+\nu}=a_\nu', \quad \{|a_\nu'|\}_0^{k-1}<1, \tag{19}$$

then $E=E_1+E_2$, *where* $E_1\subset E_0$ *is everywhere dense on* E_0, $E_2\subset E_0$ *being no more than a denumerable isolated set; if* $|a_{k-1}'|=1$, *then the single limit-points of* E *may be the arguments of the roots of the polynomial*

$$p_k(z)(1-a_{k-1})+\omega_k(z)(1+a_{k-1}).$$

Using M. Krein's arguments (2) we can get the conditions both necessary and sufficient for the set E to have the pre-assigned limit-points $\{\vartheta_r\}_1^m$; these conditions are:

$$\lim_{i,k\to\infty}g_{ik}=0, \tag{20}$$

g_{ik} being the elements of the matrix

$$\|g_{ik}\|_0^\infty=g(\|U\|),\quad g(z)=\prod_{r=1}^{m}(z-e^{i\vartheta_r}),\quad \|U\|=\|u_{ik}\|_0^\infty, \tag{20'}$$

$$u_{n-1,k}=-\bar{a}_{n-1}a_{k-1}\sqrt{\frac{h_{n+1}}{h_k}},\ (k=0,1,\ldots,n-1);\ u_{n-1,n}=\sqrt{\frac{h_n}{h_{n-1}}};$$
$$u_{n-1,k}=0,\ (k\geqslant n+1); \tag{20''}$$

* Thus, the passage from $f_\nu(z)$ to $f_{\nu+1}(z)$ consists in replacing a_i by a_{i+1} $(i=\nu,\ \nu+1,\ldots;\ \nu=0,1,\ldots)$.

** It may be proved that the function $\Phi(z)$ cannot have branch-points outside the circle.

in particular, the condition $\lim_{n\to\infty} a_n = a$, $|a| = 1$ is necessary and sufficient that the point $\theta = \pi$ be the single limit-point of E.

Theorem V. *If* $\limsup_{n\to\infty} \sqrt[n]{h_n} = 1$ (*in particular, if* $\lim_{n\to\infty} a_n = 0$), *then* E *is everywhere dense on* $<0, 2\pi>$; *if* $\liminf_{n\to\infty} \sqrt[n]{h_n} = \sin^2 \alpha$, *then the set* $e \subset E$ *of the points, where the derivative* $\sigma'(\theta) = p(\theta)$ *is positive and continuous, contains no interval of length* $> 4\alpha$; *if* $\alpha = 0$ (*in particular, if* $\lim_{n\to\infty} |a_n| = 1$), *then the set* e *is discontinuous.*

Theorem VI. *The convergence of the series* $\sum_{k=0}^{\infty} |a_k|^2$ *is necessary and sufficient for the convergence of the series* $\sum_{k=0}^{\infty} \frac{|P_k(z)|}{h_k}$ *at every point of the domain* $|z| < 1$; *under this condition is valid the asymptotic formula*

$$P_n(z) \simeq z^n \bar{\pi}\left(\frac{1}{z}\right), \quad |z| > 1, \qquad (21)$$

(*uniformly for* $|z| \geqslant R > 1$), *where* $\pi(z)$ *is an analytic function regular for* $|z| < 1$; *if the series* $\sum_{k=0}^{\infty} |a_k|$ *converges, then we have for* $|z| \geqslant 1$

$$P_n(z) = z^n \left[\bar{\pi}\left(\frac{1}{z}\right) + \bar{\varepsilon}_n\left(\frac{1}{z}\right)\right]; \quad |\varepsilon_n(z)| = O\left(\sum_{k=n}^{\infty} |a_k|\right); \quad |z| \leqslant 1; \qquad (22)$$

in this case function $\sigma(\theta)$ *is absolutely continuous and its derivative (existing almost everywhere)*

$$p(\theta) = \sigma'(\theta) = \frac{h}{|\pi(e^{i\theta})|^2}, \quad h = h_0 \prod_{k=0}^{\infty} (1 - |a_k|^2) \qquad (23)$$

is positive and continuous in $<0, 2\pi>$.

Corollary. G. Szegö [4] obtains an asymptotic formula of type (21) under condition that the function $\sigma(\theta)$ be absolutely continuous and that its derivative $p(\theta) = \sigma'(\theta)$ be positive almost everywhere; it follows that the absolute continuity of the function $\sigma(\theta)$ is not necessary.

III. Theorems IV—VI enable us to draw conclusions concerning some properties of mapping by means of C- or S-functions.

The set $E' = <0, 2\pi> - E$ is evidently the set of θ for which to the points $z = e^{i\theta}$ correspond by the mapping $w = F(z)$ the points of the imaginary axis $Rw = 0$, or by the mapping $u = f(z)$ the points of the circle $|u| = 1$, $u \neq 1$.

Theorem VII. *Under condition* (19), $E' = E_1' + E_2$, *where* $E_1' \subset E_0$ *is a discontinuous set and* E_2' *coincides with* $<0, 2\pi> - E_0^*$; *if* $|a_{k-1}'| = 1$, *then* E' *coincides with* $<0, 2\pi>$*. *If* $\limsup_{n\to\infty} \sqrt[n]{h_n} = 1$, *then* E' *is discontinuous. The conditions* (20) *are necessary and sufficient that the* C*-function have all its poles on the circle* $|z| = 1$ *with the pre-assigned limit-points* $\{z_\nu = e^{i\theta_\nu}\}_1^m$ *and no other singularities.*

If $\sum_{k=0}^{\infty} |a_k| < \infty$, *then for* $|z| \leqslant 1$ *the point* $w = x + iy = F(z)$ *does not fall off the segment formed by the straight line* $x = \frac{1}{A}$ *and the circle* $x^2 + y^2 -$

* Excluding the set of null-measure.

$-Ax=0$, *where* $A=\prod_{k=0}^{\infty}\frac{1+|a_k|}{1-|a_k|}$; *under the same conditions the point*

$$v=\xi+i\eta=zf(z)=\frac{F(z)-1}{F(z)+1} \tag{24}$$

does not fall off the lunula formed by the circles

$$\left(\xi\pm\frac{1}{A+1}\right)^2+\eta^2=\left(\frac{A}{A+1}\right)^2. \tag{25}$$

IV. To illustrate the advantage of treating C- or S-functions in connexion with the trigonometric moment-problem, consider a distribution $d\sigma(\theta)$ having the masses $\{\mu_\nu\}_1^s>0$ concentrated at the points $\{\theta_\nu\}_1^s$ and arbitrary in other respects; in this case there exist the limits

$$\lim_{z\to z_\nu}\{c_0F(z)(z-z_\nu)\}=-\frac{\mu_\nu z_\nu}{\pi}, \quad \{z_\nu=e^{i\theta_\nu}\}_1^s. \tag{26}$$

Introducing a S-function by the formula

$$f(z)=\frac{c_0F(z)-\lambda}{c_0F(z)+\lambda}, \quad R\lambda>0, \tag{27}$$

we state the existence of the limits

$$\lim_{z\to z_\nu}f(z)=1, \quad \lim_{z\to z_\nu}\frac{f(z)-1}{z-z_\nu}=\beta_\nu=\frac{2\pi}{z_\nu\mu_\nu}R\lambda, \quad (\nu=1, 2, \ldots, s); \tag{28}$$

conversely, (28) implies (26).

We come to the

Theorem VIII. *For every S-function $f(z)$ satisfying* (28) *is valid the inequality*

$$\frac{1-|f(z)|^2}{|1-f(z)|^2}\geqslant R\sum_{\nu=1}^{s}\frac{1}{z_\nu\beta_\nu}\cdot\frac{z_\nu+z}{z_\nu-z}, \quad |z|<1, \tag{29}$$

the equality sign corresponding to the function

$$f(z)=f^*(z)=\frac{c_0^*F^*(z)-\lambda}{c_0^*F^*(z)+\lambda}, \quad c_0^*F^*(z)=\frac{1}{2\pi}\sum_{\nu=1}^{s}\mu_\nu\frac{z_\nu+z}{z_\nu-z}; \tag{30}$$

in particular, for $s=1$, $z_1=1$ we come to the theorem of Julia:

$$\frac{|1-f(z)|^2}{1-|f(z)|^2}\leqslant\beta\frac{|1-z|^2}{1-|z|^2}, \quad \beta=\frac{2\pi}{\mu}R\lambda>0, \quad |z|<1. \tag{31}$$

Received
27. I. 1943.

REFERENCES

[1] J. Geronimus, C. R. Acad. Sci. URSS, XXVI, № 9 (1940); ibid., XXIX, № 1 (1940). [2] Н. И. Ахиезер и М. Г. Крейн, О некоторых вопросах теории моментов, ст. VI, Харьков (1938). [3] J. Schur, Journ. fur die reine und angew. Mathematik, 147, 205—32 (1917). [4] G. Szegö, Orthogonal polynomials, § 12. 1, New York (1939).

Comptes Rendus (Doklady) de l'Académie des Sciences de l'URSS
1943. Volume XXXIX, № 8

ASTRONOMY

ON THE STRUCTURAL FEATURES OF THE SOLAR CORONA OF SEPT. 21, 1941

By B. FESSENKOFF, Member of the Academy

During the total eclipse of September 21, 1941 the solar corona was photographed by many cameras of different length and light ratios. The most successful pictures, showing many minute details, were obtained with 5-meter coronographs of 1 : 50 light ratio. Very good photographs have also been obtained by Mrs. O. Kramer at Kamenskoe Plateau Station near Alma-Ata, by M. S. Navashin with the Saphir Boyer camera of 45-cm focal length and 10-cm linear aperture, and by other observers.

The brightness of the solar corona is known to vary enormously with the distance from the disc border. Consequently, details of the corona as a whole can be obtained only by a number of exposures, relating each to a certain zone between successive distances from the centre. It is evident that a single exposure is insufficient as a basis for arriving at any definite conclusion as to the structure of the object under consideration.

For the qualitative study of the coronal structure I have carefully examined and made drawings of the most suitable negatives taken with different coronographs. The drawings were magnified five times. All the sketches were united in one picture so as to give the structural property of the corona and not its intensity distribution. Moreover, the coronal rays; streamings and the condensation nuclei are represented with nearly the same intensity, though the real variation of their brightness may be very great. The following general features can be noted from an examination of our composite drawing.

The solar corona is composed of a great number of rays and clouds, superimposed on a continuous background. The brightness of all these features decreases rapidly, but the rate of decrease of the brightness of the rays is a little greater.

Consequently, the diffuse corona may be perceived at a distance where rays are completely absent. Measurements of Saphir Boyer plates made with a Hartmann microphotometer show that the diffuse corona corrected by the influence of the auroral ring near the horizon, as well as the halation effect, may be percieved up to a distance of 8 radii from the disc. It is to be noted that the oblateness of the isophotes does not vary, being equal at any distance to 0.2. On the other hand, the rays on the same photograph cannot be traced farther than 1.5 radii from the border. The polar rays are comparatively simple structures and are oriented nearly radially. In intermediate regions the structure is very complicated, and at first glance it seems impossible to discover any regularity. But each time the ray is sufficiently elongated, it approximates the radical direction. As good examples the negative obtained by A. A. Michailov for the purpose of testing the Einstein effect and the negative taken with the Saphir Boyer camera may be mentioned.

It is interesting to note that the intermediate regions of the corona show intense vortices, one in every quadrant. These vortices are characterized by very compli-

rated and even closed trajectories of elliptical and sometimes circular form. The heights of these vortices are of the order 0.2—0.3 of solar radii, viz. 0.20 in the SO, 0.34 in the ON and 0.32 in the NW quadrants. The vortex in the SW quadrant is situated at such a height that on the photograph taken with the Saphir Boyer camera one may easily distinguish this vortex in its fully developed form at a mean height of one radius. The most developed vortex is that situated over the group of spots which at the moment of eclipse were visible at a small distance from the border. Intensive clouds of diffuse matter, elongated branches and nearly circular trajectories of small radius are characteristic of this formation.

Moreover, numerous other details can be noticed. The coronal rays do not become more intense at the points of their intersection. In some cases the interruption of

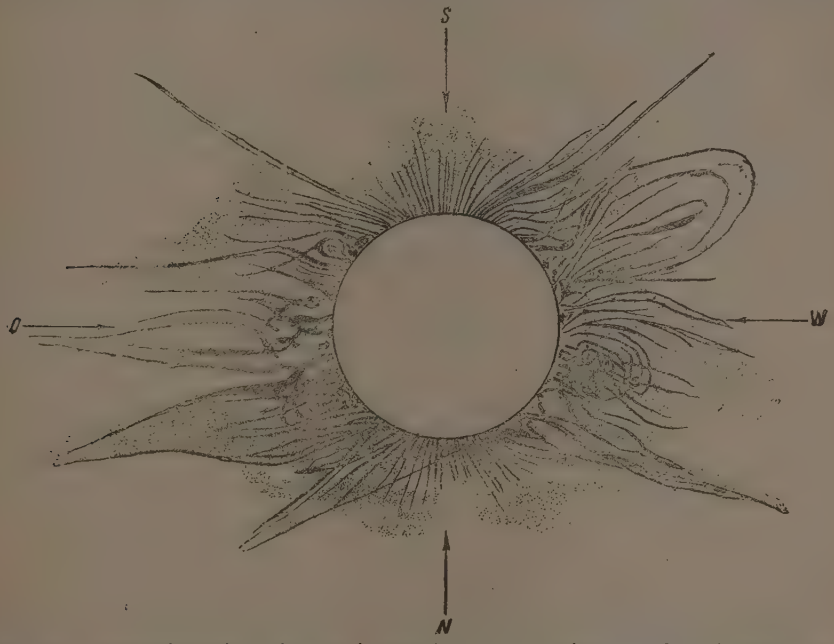

a ray and its continuation after an interval may be noticed. In 3 or 4 cases remarkable parallel currents divided by a very narrow interval are observable. The cause of these currents is not clear.

In the North Polar region a very long inclined ray tangent to the solar disc is observed. This phenomenon is very feeble and is perhaps only a border between regions of different brightness.

The solar corona seems to be a very complicated structure, consisting chiefly of separate and continuous rays which are intermingled with a generally diffused background. It is to be noted that these rays are for the most part continuous, but their contrast against the background is extremely feeble. The diminution of their brightness by 10—20% is sufficient to make them completely undetectable.

Now, this structure is a spatial one, the rays passing through a volume of a certain thickness along the line of vision. This thickness can be roughly evaluated. Taking into consideration that the brightness in the corona decreases very rapidly with the distance from the Sun's centre, for the inner corona the rate of decrease is nearly r^{-20}, but for the middle layers it slows down considerably, being r^{-5}. Simple considerations lead at once to the following formula which gives the whole thickness, contributing to the apparent coronal structure

$$S = 2r\sqrt{E^{\frac{2}{n}} - 1}$$

where n is an exponent, determining the rate of decrease, and E is a limiting contrast determining the possible visibility of the rays at certain points of the plane of the picture.

Taking $E = 10\%$ and 20%, we obtain the following value of S in terms of the radius vector

	$E = 10\%$	$E = 20\%$
$n = 20$ (the inner corona)	0.063	0.27
$n = 5$ (the middle corona)	0.394	0.548

The result is that the thickness of space, contributing to the apparent structure of the corona, increases considerably with the distance from the Sun's border. Consequently, this structure should be more complicated at greater distances from the disc of the Sun, some new rays appearing without any connexion with the former ones. In reality this is not the case. Consequently, the coronal rays must be considered as isolated phenomena produced by some active agents on the Sun and ejected into space at some angle more or less inclined to the surface. A remarkable example ([1]) of this kind is furnished by rays of extremely complicated structure, undoubtedly connected with a large group of spots near the NW part of the border of the Sun's disc, as has been mentioned above.

Institute of Astronomy and Physics.
Alma-Ata.

Received
7. IV. 1943.

REFERENCES

[1] Астрономич. журн., 19, 4, 15 (1942).

Comptes Rendus (Doklady) de l'Académie des Sciences de l'URSS
1943. Volume XXXIX, № 8

PHYSICS

INCREASE OF PHOSPHORESCENCE DURING EXCITATION

By W. W. ANTONOV-ROMANOVSKY

(Communicated by S. I. Wawilow, Member of the Academy, 29. IV. 1943)

The increase of luminescence of phosphors during excitation has not been sufficiently explored. The investigation is impeded by the presence of fluorescence, by the high velocity at which phosphorescence increases (as compared to natural decay) and by the necessity to apply complementary light filters in case excitation is due to visible light.

The phenomena that arise at the moment of excitation are more complicated than those which attend the decay of a phosphor, since both absorption and emission of light proceed at the same time.

The exciting light does not only ionize the centres of luminescence; but not infrequently it brings about a more rapid decay of the luminous power of the

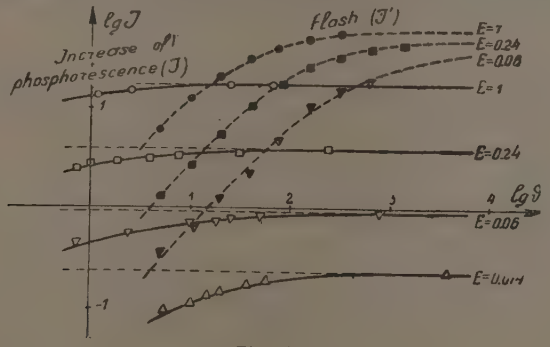

Fig. 1

phosphor. This leads to results that look rather paradoxical at first sight; it is the analysis of these results that we are concerned with in the present article.

The increase in the luminescence of an alkaline earth phosphor* at various intensities of the exciting light (illumination with the mercury line $\lambda=254$ mμ) is represented by solid curves in Fig. 1. From this figure it can be seen that the brightness of luminescence J reaches its limit value gradually and this occurs the later, the smaller E, the time being almost inversely proportional to E. As soon as excitation has ceased, J at once drops practically to zero.

The picture observed is thus analogous to that which has been described for silicate phosphors (1). Consequently, in the case considered the exciting light is at the same time a factor that accelerates the decay processes.

* The phosphor has been prepared by Z. A. Trapeznikova.

The increase of the number of recombinations may proceed along two ways. Suppose an electron to be ejected by the exciting light to a sufficiently far distance. Till the moment of the first localization, the electrons then have more probability to meet on their way some other ionized centres and unite with them.

It may also proceed under the effect of exciting light merely as a «red» one.

As has been shown by the author (1), the intensity of luminescence must gradually decrease after it has reached a certain maximum. As a matter of fact, this stands in contradiction with Fig. 1. We are thus left only the second alternative.

In this case we have (1)

$$n = \sqrt{\frac{EN}{p}} \operatorname{tg} \operatorname{hyp} (\sqrt{pEN}\,\vartheta) \tag{1}$$

and

$$J = EN \operatorname{tg} \operatorname{hyp}^2 (\sqrt{pEN}\,\vartheta), \tag{2}$$

where n is the concentration of the ionized centres; J, the intensity of luminescence; ϑ, the period of excitation; E, the intensity of the exciting light, and where the probability of recombination is

$$p = p_0 + \alpha E. \tag{3}$$

Here p_0 is the thermal probability of recombination; αE, the probability of recombination, caused by the accelerating effect of the exciting light.

As soon as the excitation ceases, the intensity of luminescence is reduced to zero, therefore $\alpha E \gg p_0$ and instead of (3) we have

$$p = \alpha E.$$

Then from (1) and (2) it follows that

$$n = \sqrt{\frac{N}{\alpha}} \operatorname{tg} \operatorname{hyp} (\sqrt{\alpha N}\, E\vartheta) \tag{4}$$

and

$$J = EN \operatorname{tg} \operatorname{hyp}^2 (\sqrt{\alpha N}\, E\vartheta). \tag{5}$$

Formula (5) shows that, in accordance with the experiment, J grows with increasing ϑ up to a certain limit which is proportional to E. The time necessary to reach this limit is inversely proportional to E.

For small values of ϑ (of the order of several seconds) the relations between the intensities for different E are no more proportional to E, but are a much more steeper function of the latter; this is a direct evidence in favour of the bimolecular nature of the process of luminescence*.

Formula (4) shows that in the case of a stabilized process ($\vartheta = \infty$) $n = \text{const}$, i. e. is independent of E. This is supported by the following experiment.

The phosphor sample was excited up to the limit with $E = 0.014$. After this the intensity of the exciting light was abruptly increased up to $E = 1$. J also attained at once the limit value, corresponding to $E = 1$. E was thereupon reduced by a sudden leap to its original value of $E = 0.014$; J also fell directly to its limit value, corresponding to $E = 0.014$.

Thus, the limit value of n_∞ does not depend on E.

It may seem that this takes place because $n_\infty = N$, i. e.; saturation being reached, no further increase is possible. However, it is no difficult matter to demonstrate, that in this case there is no saturation, and that $n_\infty \ll N$.

If along with excitation we expose the sample to the «red» light I, then the limit intensity remains the same, i. e. it does not depend upon I. This

* Under real conditions owing to the gradual weakening of the exciting light as it penetrates into the depth of the phosphor (case of a «thick» layer) we have, instead of a simple curve (5), a superposition of curves of the type (5). But since this is applicable for each separate layer, it will also hold for their sum, i. e. for the real case.

is possible only provided $n_\infty \ll N$. Indeed, if the phosphor is exposed to «red» light

$$\frac{dn}{dt} = -pn^2 + E(N-n), \text{ where } p = \alpha E + \beta I.$$

With very prolonged or so-called complete excitation $\frac{dn}{dt} = 0$, whence $(J = pn^2)$

$$J_\infty = (\alpha E + \beta I) n_\infty^2 = E(N - n_\infty). \quad (6)$$

If «red» light is eliminated, the intensity at once drops to the magnitude

$$J_{\infty E} = \alpha E n_\infty^2.$$

If it is the exciting light that is eliminated, then

$$J_{\infty I} = \beta I n_\infty^2.$$

It is obvious that $J_{\infty E} + J_{\infty I} = J_\infty$. For a thick layer an analogous picture will take place, as may be seen from experimental data (see table).

E	J_∞	$J_{\infty E}$	$J_{\infty I}$
1	1	0.11	0.9
0.24	1	0.28	0.75
0.06	1	0.45	0.55
0.014	1	0.5	0.5

Note. In the case of simultaneous exposure of phosphor to exciting and «red» light the limit intensity J_∞ is put at 1. $J_{\infty E}$ and $J_{\infty I}$ are the intensities which immediately follow the elimination of «red» or exciting light, respectively.

On the other hand, with $I = 0$ it follows from (6) that

$$J'_\infty = \alpha E n'^2_\infty = E(N - n'_\infty). \quad (7)$$

Since we find experimentally that $J_\infty \approx J'_\infty$, we obtain from (6) and (7)

$$n'_\infty = n_\infty \sqrt{\frac{\alpha E}{\alpha E + \beta I}} < n_\infty.$$

At the same time, we have from (6) and (7) $(J_\infty \approx J'_\infty)$

$$E(N - n_\infty) \approx E(N - n'_\infty).$$

This is not possible unless $n_\infty \ll N$, q. e. d.

The dotted line curves in Fig. 1 describe the initial magnitude of the flash of J' as brought about by «red» light, after excitation has ceased at a moment ϑ. The total disagreement between the runs of the dotted (J') and the solid (J) curves is striking. In the first line, for small ϑ the intensity of the flash $J' < J$; for large values of ϑ, on the contrary, $J' > J$. Secondly, the period ϑ_∞, within which the limit intensity is attained, is in the case of J' many times longer than in the case of J. Thirdly, the dependence of the limit intensity of the flash J'_∞ on E is no linear, as for J, but a much slower one.

We thus face rather paradoxical results: on the one hand, there seems to be no relation whatever between flash and luminescence during excitation; on the other hand, experiments involving simultaneous exposure to exciting and «red»

light point to that the existence of such a relation stands beyond any doubt.

The explanation lies in the fact that we deal here with a typical case of «thick» layer; which must be taken into account.

Let us suppose that the exciting light loses its intensity according as it penetrates into the depth of the phosphors, and that this proceeds according to the exponential law, i. e.

$$E = E_0 e^{-kx}. \tag{8}$$

If the excitation is a complete one ($\vartheta = \infty$), then, according to (4); the concentration of ionized centres $n_x = \text{const}$ in the external layers; only in very deep layers, when αE_x becomes comparable with p_0, n_x begins to decrease according to formula (1) ($\vartheta = \infty$).

The approximate run of E_x and n_x, as dependent on the depth of layer x, is schematically represented in Fig. 2.

As the intensity of luminescence during excitation J with constant n is proportional to E, the effective layer under these conditions is that of thickness x_E; the intensity of the exciting light decreases for this thickness several times (Fig. 2). For the flash J' it is the depth x_n that will be effective; since the «red» light penetrates to a much greater depth than the exciting light without any appreciable loss of intensity.

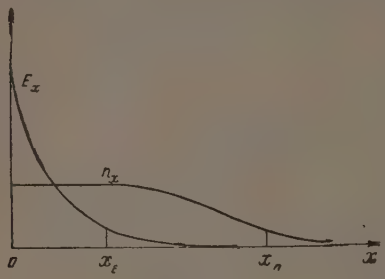

Fig. 2

Consequently, J reaches its limit value when a layer of thickness x_E is excited at full. J' does so when a layer of thickness x_n is excited, which requires a much longer period of time.

As in the case of radiation with «red» light $p = \beta I$, for a layer lying at a depth, $J_x = pn_x^2 = \beta I n_x^2$. Hence with the aid of (2) ($\vartheta = \infty$) and (8) we deduce the integral brightness of the flash $\left(J' = \int_0^\infty J_x dx \right)$

$$J' = \frac{\beta I}{\alpha k} \lg \left(1 + \frac{\alpha E_0}{p_0} \right). \tag{9}$$

In other words; in agreement with experiment (Fig. 1) we arrive at the conclusion that with full excitation the limit brightness of the flash must increase very slowly along with the increase of E.

Thus, the bimolecular scheme of phosphor luminescence; which allows for the acceleration effect of the exciting light, offers a quite satisfactory qualitative; and sometimes quantitative; interpretation of the phenomena that arise in the case of phosphor excitation.

To conclude it should be noted that; although these phenomena have a more complex character than those arising in the case of natural decay, their analysis is much easier in one respect: in the case of natural decay, displacements of the electrons proceed in the thermal way only. The length of the «free path» l and of the mean displacement ω of the electrons between the consecutive captures are comparable with the constant lattice a [2]. This excludes the possibility of applying a simple bimolecular scheme. Unlike this, during the excitation the electrons are ejected mainly in the optical way; here $l \gg a$ and $\omega \gg a$, and the simple bimolecular scheme can be successfully applied.

P. N. Lebedev Physical Institute.
Academy of Sciences of the USSR.

* Received
29. IV. 1943.

REFERENCES

[1] W. W. Antonov-Romanovsky, C. R. Acad. Sci. URSS, XXXVI, 138 (1942).
[2] W. W. Antonov-Romanovsky, Journ. of Phys., 7(1943); C. R. Acad. Sci. URSS, XXXI, 863 (1941); Труды ФИАН, 2, 2—3 (1942).

Comptes Rendus (Doklady) de l'Académie des Sciences de l'URSS
1943. Volume XXXIX, № 8

GEOPHYSICS

SCATTERED RADIATION OF CLOUDLESS SKY

By N. N. KALITIN

(Communicated by A. A. Grigoriev, Member of the Academy, 29. I. 1943)

The magnitude of the intensity of the scattered radiation of a cloudless sky is determined by the height of the Sun above the horizon, the transparency of the atmosphere, its optical heterogeneity, and the albedo of the Earth surface. Prull has proposed a formula by means of which the magnitude of the scattered radiation of cloudless sky can be related to the coefficient of turbidity of the atmosphere B (for λ ranging from 3000 A to 7000 A); Bork ([1]) studied scattered radiation of the

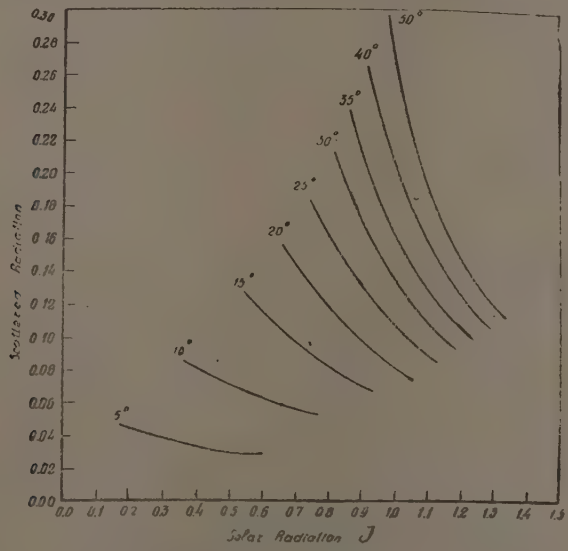

Fig. 1. Relation between I and i for various heights of Sun

integral flow, as dependent on the factor of turbidity T. It seems of practical interest to find the relation existing between the magnitude of the integral flow of scattered radiation of the atmosphere and the data of measurements of the intensity of solar radiation. From this relation it will be possible to obtain the magnitude of scattered radiation without performing direct measurements of the latter, from a mere knowledge of the intensity of solar radiation.

In order to obtain the relation between those two magnitudes of radiation, we subjected to treatment the records taken with Yanishevsky's pyronograph and with the actinograph at Slutzk for a period of 5 years.

To the treatment were subjected records for those days when the sky was cloudless either throughout the day, or from sunrise or sunset to midday. In the final treatment of the material only those records were taken into account which refer to days when the Sun was 30° above the horizon and higher, and when there was no snow covering. In the course of 5 years there were no more than 127 such days, and it is from the treatment of the respective records that the conclusions given below have been derived.

The treatment consisted in plotting the magnitudes of intensity of the scattered radiation i and of the solar radiation I upon the perpendicular surface for each 5° of the height h of the Sun beginning with an altitude of 5° and up to 50°. A total of 480 magnitudes was obtained, expressing the relation between i and I for various heights of the Sun and various magnitudes of the coefficient of atmosphere transparency p. The material treated was classed into five groups according to the magnitudes of transparency for the mean values of p: 0.85; 0.80; 0.75; 0.70; 0.65 (for a Sun height of 30°).

From the results obtained it is obvious that in the case of small Sun altitudes the magnitude of scattered radiation grows but little with decreasing atmosphere

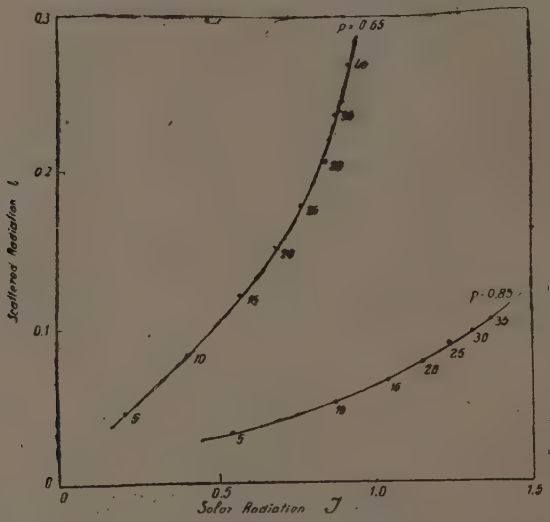

Fig. 2. Ratio of I to i with the coefficient of atmosphere transparency $p=0.85$ and $p=0.65$ and for various heights of Sun

transparency. In the case of great altitudes of the Sun the increase of i along with decreasing atmosphere transparency proceeds much more intensely. This relation is brought out in Fig. 1; along the axis of abscissae are plotted the magnitudes of I; along the axis of ordinates, the magnitudes of i. The curves reproduce the heights of the Sun, which is also expressed in respective figures.

The degree of variation of i for different heights of the Sun, as dependent upon the variation of atmosphere transparency, is evident from the following considerations: with a p equal to 0.65 and a Sun altitude of 5°, the magnitude of i is equal to 0.048 cal., while with a height of 50° the magnitude of i is found to be 0.290 cal. With a p equal to 0.80 for a height of 5° of the Sun i is equal to 0.330 cal.; and for a Sun height of 50° it amounts to 0.123. In the former case the ratio of the magnitude of scattered radiation with 50° to that with 5° of Sun height equals 6.0, in the latter 3.7.

Fig. 2 shows the relation between the intensities of the solar and the scattered radiation for the two extreme cases, viz. for very good atmosphere transparency,

$p = 0.85$, and for poor transparency, $p = 0.65$. The figures plotted against each point express the height of the Sun above the horizon.

As an ultimate result of the work performed there was plotted a table; knowing at the moment of measuring the magnitude of the intensity of solar radiation I and the altitude of the Sun h, it is possible to find with the aid of this table for this moment, without any measurement, the magnitude of intensity of the scattered radiation of the atmosphere.

Intensity of Scattered Radiation with Cloudless Sky as Dependent on Height of Sun h and Magnitude of Intensity of Solar Radiation I Falling on a Perpendicular Surface

h \ I	0.1	0.2	0.3	0.4	0.5	0.6	0.7	0.8	0.9	1.0	1.1	1.2	1.3	1.4
4°		35	28											
6°			50	42	37									
8°			75	62	53	47								
10°				88	72	61	54							
12°					97	80	68	61						
14°					123	103	87	74	65					
16°						125	105	88	74					
18°						149	122	101	85	73				
20°							144	118	98	81				
22°							167	136	111	91	76			
24°								156	125	101	83			
26°								175	140	113	92			
28°								196	153	123	101			
30°									168	135	109	88		
32°									190	147	118	97		
34°									207	162	129	105		
36°									225	175	139	112		
38°									245	190	149	120	99	
40°										207	160	127	105	
42°										223	173	136	111	
44°										235	183	146	117	
46°										246	193	153	124	
48°										260	205	162	131	
50°										276	216	173	139	114

In the table the magnitudes of intensity of scattered radiation of the atmosphere are expressed in thousandths of calories; the magnitude of I is expressed in tenths of calories, and h is given at two degree intervals.

Making use of this table, it is possible to find from the magnitude of I, measured with the aid of an actinometer, within the scope of magnitudes most frequently met in practice, the value of i. Hence the total radiation may also be found, if necessary, by transferring I onto a horizontal plane.

All the magnitudes of radiation given above are expressed according to the usage adopted in this country, in units of the European scale.

It would seem desirable to extend this table towards greater Sun altitudes, and towards both greater and smaller magnitudes of atmosphere transparency; it is the latter case that seems to be the most promising. This will not be practicable unless we have at our disposal observational data collected at a point situated more southerly than Slutzk. It is also necessary to dispose of a larger number of observations, which will make the results obtained more accurate.

The influence upon i of the albedo of snow covering at various altitudes of the Sun should also be investigated.

Received
29. I. 1943.

REFERENCES

[1] Н. И. Б о р к, Метеорология и гидрология, 1 (1941).

Comptes Rendus (Doklady) de l'Académie des Sciences de l'URSS
1943. Volume XXXIX, № 8

APPLIED HYDROMECHANICS

ON THE WORKING OF SUPERCAVITATING SCREW PROPELLERS

By V. L. POSDUNINE, Member of the Academy

By supercavitating screw propellers I mean ship-propellers working at such a stage of cavitation that near the leading and trailing edges of the screw blades, at their rear, a separation of the flow takes place, and what has been a continuous flow of water in front of the screw breaks down within the screw into several free jets corresponding quantitatively to the number of blades. In and behind the screw these jets flow in a space filled with a mixture of air and water vapour. It is supposed, moreover, that by virtue of inertia the flow is not restored to integrity until after some distance behind the screw is passed. Such screws are also described as completely cavitating screws or screws with separation of the streamlines.

In my paper entitled «A to-day problem in the field of ship-propellers» (1) a historical analysis of the development of ship screw constructions and the results of experimental work with elementary cavitating screw models, carried out in 1940, partly in 1941, both went to show that the phenomenon of supercavitation opens wide prospects for new designs in the domain of ship-propeller construction, whereby the rotation number can be increased considerably. In the present note the work of supercavitating propellers is considered in the theoretical light, so as to reveal the essentials of the operation of such screws and furnish a basis for the elaboration of a complete theory of action and construction of supercavitating screw propellers.

We proceed further from the following statements and assumptions:

1. The operational differences between supercavitating and ordinary non-cavitating propellers are so great in point of physical phenomena that no common theory of operation or single type of construction will suit the two kinds of screw.

2. The propellers operate in a free flow of water, undisturbed by the presence of the ship. The fluid is supposed to be perfectly incompressible and inviscid.

3. The work of supercavitating screws is studied on the conception of separation in the plane problem, since the three-dimensional problem of streamline flow with separation remains unsolved at all for the time being.

By analogy with the simple streamline theory of ordinary propellers we here confine ourselves to the hypothetical case when the screw works without curling up of the flow. We shall first try and create a hydromechanical model of such propellers.

To Sir Charles Parsons (2), an eminent English engineer, belongs the credit for having given a most valuable description of the operation of cavitating propellers, which is quite unique as regards clearness of representation and depth of insight into the essence of the phenomena involved in the operation of these screws. We find it in his report concerning the use of turbine steam-engines on ships, delivered at the Institution of Naval Architects in 1897.

The picture drawn by Parsons is based upon two-year laboratory work on the problem of cavitation of screw propellers, which was started in connexion with the difficulties that arose from an attempt to use propellers with a high rotation

number on the first turbine steam-engine ship «Turbinia». This ship, though an experimental construction, has her name inscribed on the records of ship-building history. The laboratory tests were made on screw models about 50 mm (2″) in diameter in a tank filled with water heated nearly to boiling, the prototype of the low pressure water tunnels of to-day. It should be emphazised that these tests were run in undisturbed water when no forward movement was made by the propeller. The formation of cavities and the development of their outline and shape with increasing number of screw revolutions was visualized by means of a stroboscope.

It is well here to quote some results of Parsons' observations which are of direct interest for the following.

«It appeared that a cavity or blister first formed a little behind the leading edge and near the tip of the blade; then, as the speed of revolution was increased, it enlarged in all directions, until, at a speed corresponding to that in Turbinia's propeller, it had grown so as to cover a sector of the screw disk of 90°. When the speed was still farther increased, the screw, as a whole, revolved in a cylindrical cavity, from one end of which the blades scraped off layers of solid water, delivering them into the other. In this extreme case nearly the whole energy of the screw was expended in maintaining this vacuous space. It also appeared, when the cavity had grown to be a little larger than the width of the blade, that the leading edge acted like a wedge, the forward side of the edge giving negative thrust».

A similar picture and in a very striking form, too, was observed by myself in the above-mentioned experiments on narrow-blade models with wedge-shaped blades. The only difference was that with a high number of revolutions and a low value of the cavitation number the vacuous cylindrical space, pierced through by independent spiral jets, was removed so far away behind the propeller that it was not always possible under the available system of windows in the low pressure water tunnel to observe the fusion of jets shed by the screw and the consequent restoration of the flow's integrity. This departure from the picture described by Parsons may be entirely accounted for by the fact that our experiments were run in a stream of water moving at the same speed with which the propeller moved forward, whereas Parsons' experiments were made in undisturbed water. So it will be apparent that our results are in no contradiction to his, but rather complement them. Considering the totality of phenomena observed in the described tests under conditions of supercavitation, one is led to conclude that screws working in accordance with the above description can really give a thrust, owing to the reaction of the cast off jets, even if they work without forward motion in the face of a certain negative thrust on the leading edges of the blades, which creates a drag at the inflow of the water to the propellr.

Plainly enough, supercavitation screws operate quite differently from non-cavitating screws. For that reason the sections of their blades should have their proper form and orientation with respect to the flow of water. Now,on the basis of all that has been said here, it is not difficult to form a hydromechanical model representing the work of supercavitating propellers.

Let us replace the supercavitating propeller by a disk of infinitesimal thickness and equal in diameter to the propeller. In accordance with the conceptions of Reissner ([3]), Lanchester ([4]) and others we suppose this disk to shed water jets backwards by periodical impulses instead of being endowed with a smooth and continuous action on the fluid, which a similar disk (actuator) is assumed to have according to the streamline theory of Rankine-Froude. Suppose further that our actuator disk, disturbing suddenly the integrity of the incoming flow of water, is able to break it into jets of such thickness that the pressure within them may be regarded as invariable throughout their thickness and equal to the pressure at their free surfaces. It will be obvious that in the propeller not only the velocity of water, but also its pressure are subject to leap-like variations.

The scheme shown in the figure brings out all variations of the velocity and pressure in a flow of water before, within, and behind the propeller. In this scheme

the following notation is adopted: DD, the plane of screw disk; p_0 and v_0, the pressure and, respectively, velocity of the water at an infinite distance before the screw; p and v, the same quantities directly before the screw; Δp and Δv, the leap-like increment of pressure and velocity, respectively, within the screw; p_d and v_d, the pressure and velocity of water behind the screw, p_d being obviously equal to the pressure of water vapour.

The latter quantities remain constant throughout the length of the jets produced to infinity, which fact is in accordance with the properties of Helmholtz-Kirhoff's flow with separation and also conforms to the operation of supercavitating propellers as outlined above.

The most characteristic feature of the hydromechanical model of work of supercavitating propellers is a negative jump instead of a positive one observed in the case of non-cavitating propellers according to the scheme of Froude.

The hydromechanical model of the operation of supercavitating screws thus constructed may serve as a basis for solving some fundamental problems of the theory of screw propellers, such as the determination of the velocity of water inflow

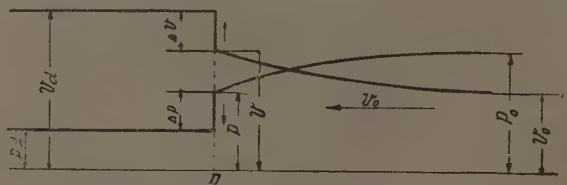

Scheme of velocity and pressure variation

to the screw under the conditions of fully developed cavitation, or of the thrust-value, or of the efficiency of supercavitating screws. Below, the solution of these problems is given irrespective of the construction of the supercavitating propeller, though our hydromechanical model contains all the principal data for establishing definite relations between the conditions of operation and structural elements of a supercavitating screw.

Now we turn to what is the most important question in the theory of any screw propeller, viz. to the determination of the velocity of the water inflow to the screw. In accordance with the figure Bernoulli's integral for the flow of water before the screw may be written in the following form:

$$\frac{v}{v_0} = \sqrt{1 + \frac{p_0 - p}{\frac{1}{2}\rho v_0^2}} = \sqrt{(1 + \sigma_0) - \frac{\Delta p}{\frac{1}{2}\rho v_0^2}}, \qquad (1)$$

where $\sigma_0 = \frac{p_0 - p_d}{\frac{1}{2}\rho v_0^2}$ is the cavitation number, a characteristic of the external flow; ρ, mass density of water; $\Delta p = p - p_d$, jump of pressure in the screw.

Adopting the simplest relation between Δp and Δv, corresponding to a sudden change of the cross-section area of the flow upon its disintegration in the screw, $\Delta p = \frac{1}{2}\rho(\Delta v)^2$, we can write Bernoulli's integral (1) in the following form:

$$\frac{v}{v_0} = \sqrt{(1 + \sigma_0) - \left(\frac{\Delta v}{v}\right)^2 \left(\frac{v}{v_0}\right)^2}. \qquad (2)$$

Solving this equation with respect to $\frac{v}{v_0}$, we have

$$\frac{v}{v_0} = \sqrt{\frac{1 + \sigma_0}{1 + \left(\frac{\Delta v}{v}\right)^2}}. \qquad (3)$$

From this formula a set of interesting and important conclusions of the operation of supercavitating screw propellers can be made. First of all, formula

(3) may not be applied to the propeller as a whole unless we assume that $\frac{\Delta v}{v} = \text{const}$ along the radius of the propeller.

However this value varies along the radius being connected for a given number of blades with the shape, size and inclination of separate blade-sections which are all variable with the radius. In the selection of these elements of the screw the constructors have a certain freedom of choice. Therefore the value $\frac{\Delta v}{v}$ is a parameter of the relation between the conditions of operation of a supercavitating screw and its construction.

Furthermore, it follows from formula (3) that $\frac{\Delta v}{v} = \sqrt{\sigma_0}$ is a critical value of the parameter, for which the velocity of inflow to the screw v becomes equal to the forward motion of the latter, v_0. It is also apparent that with $\frac{\Delta v}{v} < \sqrt{\sigma_0}$ the velocity of inflow is larger than and with $\frac{\Delta v}{v} > \sqrt{\sigma_0}$ is smaller than v_0.

At the first sight it seems rather strange that there are cases when the velocity of inflow to a screw working under conditions of fully developed cavitation may possibly diminish. I, however, on one occasion happened to observe this phenomenon; this was by the end of February 1941 while testing my cavitating screw-model No. 758 in a low-pressure water tunnel. I then found that with small values of $\sigma_0 < 0.5$ the normal increase of thrust with increasing rotation number of the model was attended by a very appreciable decrease of the inflow velocity, and this was the more pronounced, the lower the value of σ_0 and the larger the number of revolutions of the model. In the literature concerned with screws working under circulation there is one paper by Bauersfeld (6), which points out the theoretical possibility of this phenomenon.

Turning to the question of the determination of the theoretical thrust S in the case of a supercavitating screw, we shall place the control surfaces directly before and behind the screw. Making use of the law of momentum, we may write the following expression for the value of S conformably to the nature of the operation of the screw and to the drawing in the figure:

$$S = m\Delta v - F\Delta p = m\left(1 - \frac{1}{2}\frac{\Delta v}{v}\right)\Delta v. \qquad (4)$$

Here $m = \rho F v$ is the mass of inflowing water per unit time; F, area of the screw disk; Δp, jump of pressure; $\Delta p = p - p_d = \frac{1}{2}\rho(\Delta v)^2$.

By means of formula (3) and the notation of formula (4) we can write the expression for S in the form

$$S = (1 + \sigma_0)\frac{\left(1 - \frac{1}{2}\frac{\Delta v}{v}\right)\frac{\Delta v}{v}}{1 + \left(\frac{\Delta v}{v}\right)^2}\rho F v_0^2. \qquad (5)$$

In writing down the expressions (4) and (5) it was supposed that $\frac{\Delta v}{v} = \text{const}$ all over the area of the screw disk, on the strength of the considerations expressed earlier in analysing formula (3). It is seen from formula (5) that the assumption corresponds to a uniform distribution of the thrust over the whole area of the disk.

For analysing the quantity S, we shall have recourse to the customary notion of specific load coefficient of the screw $\zeta = \frac{S}{\frac{1}{2}\rho F v_0^2}$. Putting for brevity sake $\zeta = k(1 + \sigma_0)$ and $\frac{\Delta v}{v} = y$, formula (5) can be rewritten in the form of the following equation:

$$(1 + k)\, y^2 - 2y + k = 0.$$

The solution of this equation is given by the following expression for the parameter $\frac{\Delta v}{v}$:

$$\frac{\Delta v}{v} = \frac{1 - \sqrt{1 - k(1+k)}}{1+k}. \tag{6}$$

From that formula it is evident that the parameter $\frac{\Delta v}{v}$ takes real or imaginary values, according as k is $\leqslant 0.62$ or > 0.62.

Replacing the parameter $\frac{\Delta v}{v}$ by the coefficient of jet contraction in the screw $\varepsilon = 1 : \left(1 + \frac{\Delta v}{v}\right)$, we, by means of simple computations, come from what has been said here to the conclusion that the maximum real value of the specific load coefficient is $\zeta = 0.62(1+\sigma_0)$ for $\varepsilon = 0.62$, i. e. for the so-called perfect contraction of jets. The minimum value $\zeta = 0$ corresponds to $\varepsilon = 1.00$, i. e. to the case when there is no contraction of jets and, accordingly, no breakdown of the flow. For all intermediate values of ζ the supercavitating screw will apparently work within the limits of the inequality $0.62 < \varepsilon < 1.00$, which indicates the so-called incomplete contraction of the jets.

In that way the applicability boundaries of the theory exposed above are set up, and it turns out that under conditions of an ideal fluid the theory breaks down on the transition to ordinary non-cavitating screw propellers. The zero value of the thrust in the absence of separation has much the same meaning as the famous paradox of Euler, which states that no resistance is offered by a body to the motion of an ideal fluid. The imaginary values in the solution of the problem considered here lead one to suppose that outside the limits of the perfect contraction of jets the operation of the screw propeller is attended by some phenomena that have not yet been revealed by us.

To end with, we shall consider the question as to the ideal efficiency of supercavitating screws η. This quantity can, in accordance with the stated conception of the nature of operation of such screws, be treated as the ratio of the useful work of the thrust S, as given by formula (4), at the velocity v_0 to the work of the maximum possible thrust S_{max} at the same velocity under abstract condition when the negative part of the thrust in formula (4) is supposed to be absent. Then, in accordance with this formula, we have:

$$\eta = \frac{S}{S_{max}} = 1 - \frac{1}{2}\frac{\Delta v}{v}. \tag{7}$$

The conclusions to be drawn from the present analysis of the operation of supercavitating screw propellers under ideal conditions are as follows:

1) The value of the specific load coefficient of supercavitating screws varies from 0 to 0.62 $(1+\sigma_i)$ securing a sufficiently wide range of application of these screw propellers in practice.

2) The value of the thrust, varying directly as $1+\sigma_0$, is diminished with decreasing cavitation number σ_0, but does not vanish even for $\sigma_0 = 0$, i. e. when the ship is moving at an arbitrarily high speed.

3) The value of the ideal efficiency of supercavitating screws, ranging from 0.69 to 1, is dependent solely upon the coefficient of specific load ζ and does not appear to depend upon the cavitation number σ_0.

These conclusions are in fairly good agreement with the experimental results obtained with our models of supercavitating screw propellers.

Received
10. V. 1943.

REFERENCES

[1] В. Л. Поздюнин, Сов. наука, 2 (1941). [2] Ch. Parsons, Trans. Inst. of Nav. Arch., 38 (1897). [3] Reissner, ZS. f. Flugtechnik u. Motorluftschiffahrt (1910, 1911, 1912). [4] F. W. Lanchester, Trans. Inst. of Nav. Arch., 57 (1915). [5] Bauersfeld, VDI, 66, 21 (1922).

Comptes Rendus (Doklady) de l'Académie des Sciences de l'URSS
1943. Volume XXXIX, № 8

CHEMISTRY

ON ADDITION PRODUCTS OF DIENES TO TOLUENE

By B. A. ARBUSOV and E. V. KUZNETZOV

(Communicated by A. E. Arbusov, Member of the Academy, 22. II. 1943)

In numerous patents( ) it is pointed out that certain aromatic hydrocarbons can react with diolefins under the action of sodium. Thus, butadiene yields with toluene phenyl-1-pentene-3, b. p. 203—204°. Isoprene and 2, 3-dimethylbutadiene also react with toluene. No details have been reported on the isolated compounds.

The chemism of the processes taking place in these reactions has been explained by the works of K. Ziegler. This author has demonstrated that organometallic compounds are added to dienes. According to Ziegler's experiments, the addition product of one molecule of butadiene to benzyl lithium has the structure of a 1 : 4 addition product. The next butadiene molecules are added partly in position 1:2. Ziegler used in his experiments benzyl lithium itself and did not isolate the addition products of butadiene, but hydrogenated directly the reaction mixture and separated phenyl paraffins.

Addition products of dienes to aromatic compounds are of considerable interest and can be used as initial products for the synthesis of various compounds and, in particular, of hydroaromatic compounds through cyclization.

In the present paper data are reported on the products obtained in the reaction of butadiene with toluene in the presence of sodium, and their cyclization, according to Bogert (²), is described.

In the carrying out of the reaction between toluene and butadiene the deciding factor is the degree of dispersion of sodium. The finer sodium is dispersed, the higher the yield of the addition products of butadiene to toluene.

The best results have been obtained under the following conditions (the reaction was carried out in a steel autoclave): toluene 300 g, butadiene 200 cm³, sodium as a fine dust 15 g, temperature of heating 90°, time of heating 10 hrs, maximum pressure in the autoclave 5 atm., yield of fraction 80—220°/16 mm 142 g. In cases when sodium was badly dispersed, under the same conditions the yield of fraction 80—220°/16 mm decreased to 20—30 g.

Through distillation of the broad fraction 80—220°/16 mm products of addition to toluene of one molecule of butadiene (I), two molecules of butadiene (II), three molecules of butadiene (III) and four molecules of butadiene (IV) were isolated. The amounts of the corresponding products were I—50%, II—27%, III—20%, IV—3% with respect to the weight of the broad fraction used.

The properties of the isolated products are tabulated below.

	B. p. at 16 mm, °C	n_D^{21}	d_{21}^{21}	*MR* calcd.	*MR* found
I. $C_6H_5CH_2(C_4H_6)H$	92 - 94	1.5090	0.876	F_4 49.1	49.2
II. $C_6H_5CH_2(C_4H_6)_2H$	140—142	1.5105	0.889	F_5 67.1	67.0
III. $C_6H_5CH_2(C_4H_6)_3H$	188—191	1.5125	0.898	F_6 85.2	85.0
IV. $C_6H_5CH_2(C_4H_6)_4H$	210—220	1.5135	0.920	F_7 102.94	—

Analyses of the Products Obtained

Products	Weighed portion	CO_2	H_2O	Calculated		Found	
				C	H	C	H
I. $C_{11}H_{14}$	—	—	—	—	—	—	—
II. $C_{15}H_{20}$	0.1250	0.4012	0.1168	90.0	10.0	89.9	10.3
III. $C_{19}H_{26}$	0.1143	0.3756	0.1248	89.7	10.3	89.5	10.5
IV. $C_{23}H_{32}$	0.1283	0.4195	0.1096	89.6	9.4	89.4	9.5

All the compounds obtained, when oxidized with $KMnO_4$, yielded benzoic acid, this showing that the butadiene had been added to the methyl group of toluene.

Phenyl-1-pentene-3 (I) was subjected to cyclization according to Bogert with 90% sulphuric acid, and α-methyl-tetraline was obtained, b. p. 153—155°/55 mm; yield 95%.

Dehydrogenation of α-methyl-tetraline with sulphur yielded α-methyl-naphthalene (75%) having the following constants: b. p. 145°/55 mm; $n_D^{20} = 1.6130$; $d_{20}^{20} = 1.001$; $C_{11}H_{10}F_5$, MR calcd. 48.99, found 49.37.

Exaltation of the naphthalene nucleus was accepted as 2.73.

Accordingly, the cyclization reaction follows the scheme

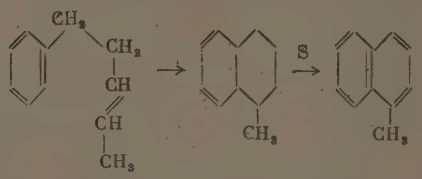

α-methyl-naphthalene obtained is of high purity and gives a picrate having without crystallization m. p. 141—142°, this corresponding to the melting point of the pure picrate of α-methyl-naphthalene.

The second product of condensation with butadiene (II) (9-phenyl-nonadiene-2, 6) when cyclized according to Bogert yielded a hydrocarbon with the following constants (yield 90%): b. p. 162—164°/18 mm; $n_D^{17} = 1.5471$; $d_{71}^{17} = 0.986$; $C_{15}H_{20}F_2$, MR calcd. 63.66; MR found 64.3.

The data of molecular refraction point at the formation of two cycles with the disappearance of two double bonds.

To the cyclization product the structure of a hydrogenated benzonaphthene of a hydrogenated phenanthrene can be ascribed:

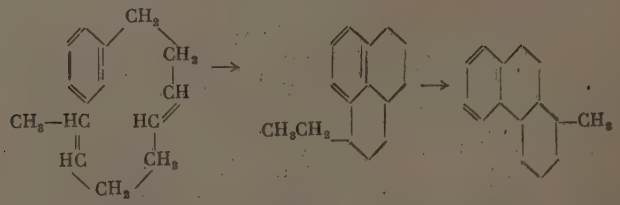

Attempts to dehydrogenate with sulphur the product obtained gave no positive results, hydrogenated benzonaphthene seems therefore to be the more probable structure, though further confirmation is needed.

The addition product of 3 molecules of butadiene to toluene was also subjected to cyclization.

Tetraline, like toluene, enters into reaction with butadiene, as described in the patent.

The addition product of the molecule of butadiene to tetraline, isolated by us; had the following constants: b. p. 140—142°/16 mm; $n_D^{21} = 1.5378$; $d_{21}^{21} = 0.953$; $C_{14}H_{18}F_4$, MR calcd. 60.58, found 60.92.

The yield of the product (at 160°) was 15% calculated to the weight of the butadiene taken. Its cyclization according to Bogert gave a substance having the following constants: b. p. 148—150°/16 mm; $n_D^{21} = 1.5548$; $d_{21}^{21} = 1.0008$; $C_{14}H_{18}F_3$, MR calcd. 58.85, found 59.2. 0.1500 g of substance, 0.4954 g CO_2, 0.1355 g H_2O; $C_{14}H_{18}$ calcd. C—90 32%, H—9.68%; found C—90 1%, H—10.04%.

The yield of the cyclization product was 85%. Its dehydrogenation with sulphur led to the formation of a resin, this being in favour of the benzonaphthene nature of the cyclization products:

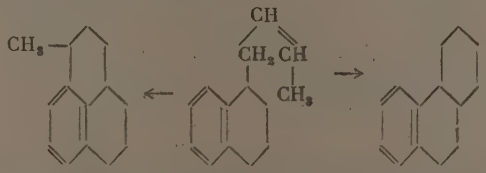

Conjugated diene systems substituted at the ends react with toluene by far not so readily. Thus, 300 g of toluene and 250 g of hexadiene-2, 4 (isolated from the by-products of synthetic rubber industry) (b. p. 78—83°) were heated with 20 g of finely dispersed sodium in an autoclave at 70° for 10 hrs. After decomposition with water and distillation 40 g of the addition product of hexadiene to toluene were isolated.

6-phenyl-5-methyl-hexene-3

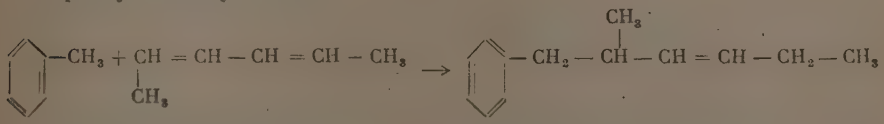

is an oily liquid with a peculiar smell and has the following constants; b.p. 106—110°/16 mm; $n_D^{21} = 1.4905$; $d_{21}^{21} = 0.875$; $C_{15}H_{18}F_4$; MR calcd. 58.16, found 57.86. 0.1703 g of substance, 0.5600 g CO_2; 0.1600 g H_2O; $C_{13}H_{18}$ calcd. C = 89.65, H = 10.34; found C = 89.67, H = 10.42.

The further study of the addition products of dienes to aromatic compounds and their cyclization is under way.

Chemical Technological Institute.
Kazan.

Received
22. II. 1943.

REFERENCES

[1] Hoffmann u. Michael, герм. пат. 557514 (1928); швейц. пат 144850 (1928); Chem. Cbl., II, 1055 (1931); англ. пат. 315312 (1929); франц. пат. 667748 (1928); Chem. Abs., 24, 3247 (1930). [2] M. Bogert, Journ. Am. Chem. Soc., 56, 919 (1934). [3] Lessner, Lieb. Ann., 402, 10 (1914).

Comptes Rendus (Doklady) de l'Académie des Sciences de l'URSS
1943. Volume XXXIX, № 8

CHEMISTRY

STUDIES ON SOLUBILITY OF CARBON IN SILICOMANGANESE

By N. N. KURNAKOV

(Communicated by N. P. Chizhevsky, Member of the Academy, 15. XII. 1942)

Silicomanganese is an alloy containing 50 to 65% Mn, 10 to 20% Si, up to 1.2% C and the remainder is iron, phosphor, sulphur, etc. It serves for the production of low-carbon ferromanganese (80% Mn, 1% C) and is also employed for dioxidizing steel. Carbon in silicomanganese is an undesired impurity which cannot, however, be removed entirely.

As a result of investigation by Doerinckel (1), Lebeau (2,3), Gin (4), Baraduck-Muller (5), Frilley (6), Boren (7), the alloys of manganese and silicon with up to

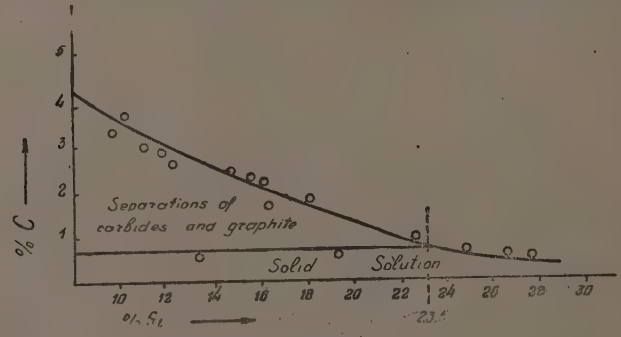

Content of carbon in silicomanganese as dependent upon content of silicon

35% of silicon are known to contain the following silicides of manganese: Mn_2Si, Mn_5Si_2, Mn_2Si_3, MnSi and others. Of these compounds, only monosilicide of manganese MnSi leaves no doubt. The ternary system Mn—Si—Fe has been investigated by Vogel and Bedarf.

Data on solubility of carbon in manganese-silicon alloys with 60 to 70% manganese, as reported by Jillet and Williams (8) and Durrer (9,10), show that with 18% Si the content of carbon is about 1%.

The alloys to be studied were made of Kahlbaum's aluminothermal manganese (96% Mn), of silicon from the plant of Cheliabinsk (98% Si), and of Armco iron. The smelting process was carried on in clay crucibles in a high-frequency electric furnace. Carbon was introduced in the form of ferromanganese (77.92% Mn, 4% C). In order to clear up the conditions under which the absorption of carbon takes place, part of the alloys was prepared in graphite crucibles. The results of chemical analyses are listed in Table 1 and the figure. The microstructure of the alloys was studied after etching the thin-sections with Baraduck-Muller's reagent (5), a solution of one volume of hydrofluoric acid in two volumes of alcohol.

Table 1

Solubility of Carbon in Silicomanganese

Nos. of alloys	C, %	Si, %	Mn, %
13	3.15	9.87	62.12
G-10	3.37	10.30	—
310	2.87	11.47	58.87
G-13	2.8	12.16	61 88
10	2.59	12.22	59.66
15	2.31	14.69	58.09
311	2.23	15.91	55.81
19	2.13	16.33	58.20
CA-13 bis	1.71	16.66	57.77
G-22	1.77	18.15	—
K-22	1.2	23.17	51.77
G-25	0.8	25.0	—
G-24	0.71	27.0	—
G-23	0.62	27.93	—

Note. Alloys denoted by G were smelted in graphite crucibles.

The description of the microstructure is summarized in Table 2.

The investigation of graphite in thin-sections is a matter of considerable difficulty, because of the crumbling of laminae of graphite, etc., which fact was described by Morrough ([12]). Therefore a binocular microscope was used for the

Table 2

Summary of Microstructure Data

Nos. of alloys	C, %	Si, %	Mn, %	Fe, %	Notes
G-10	3.37	10.3	67.88	—	Needles and separations of carbides
A-10	0.12	11.89	69.22	18.69	No carbide needles
G-13	2.8	12.16	61.88	—	Many carbide needles
CA-12	0.47	13.06	—	—	No carbide needles
19	2.43	18.33	58.20	—	Carbide veinlets, eutectic separations
A-17	0.79	18.8	—	17.40	No separation of carbide, eutectic
K-22	1.2	23.17	51.77	—	Thin carbide needles
G-25	0.8	25.0	—	—	Homogeneous fields, no needles
G-23	0.62	27.93	51.15	—	Homogeneous dissected fields; no separation of carbide
A-30	0.22	31.8	47.88	15.3	Eutectic

Note. Letter G indicates alloys smelted in graphite crucibles.

examination of the separated graphite in our alloys. This was carried out by E. S. Burova. The graphite had separated in the form of hexagonal opaque tablets (Table 3).

The result of these investigations was a solubility curve of carbon in silicomanganese (see figure), which showed that in the alloys with 10—23.4% Si and 0.8—3.5% carbon the latter was present in the form of typical primary needles which were separations of double carbides of iron and manganese, $nMn_3C \cdot nFe_3C$, and also in the form of separations of graphite. This composition of the double carbides was confirmed by a later work of P. I. Khitarov([11]). If its con-

Table 3

Summary of Data on Graphite Separations

Nos. of alloys	Si, %	Graphite separations
G-13 bis	14.89	Graphite forms a nest within the alloy
G-15 bis	15.41	Graphite in the interior of the alloy
G-18 bis	19.62	Many separations of graphite within the alloy
G-18	20.68	Much graphite within the alloy
G-24 bis	23.55	No separation of graphite

tent was below 0.8%, then carbon, irrespective of the content of silicon, was always found to form a solid solution.

Thus, in order to obtain a silicomanganese with 1% C one should have no less than 23.5% Si in the alloy.

Institute of General and Inorganic Chemistry.
Academy of Sciences of the USSR.

Received
15. XII. 1942.

REFERENCES

[1] Doerinckel, ZS. anorg. allg. Chem., **50**, 117 (1906). [2] Lebeau, C. R, **136**, 233 (1903). [3] Lebeau, C. R., **143**, 1229 (1906). [4] Gin, C. R., **144**, 85 (1907). [5] Baraduck-Muller, Rev. Met., **7**, 737 (1910). [6] Frilley, Rev. Met., **8**, 468 (1911). [7] Boren, Ark. f. Kem. Min. o. Geol. **11**, 423 (1933). [8] Jillet and Williams, Bureau of Mines, Bull. №. 173, Manganese, 157 (1920). [9] Durrer, Stahl u. Eisen, **43**, 696 (1923). [10] Гейгер, Литейное дело, статья Дюррера, **1**, 59 (1934). [11] П. И. Хитаров, Двойные карбиды железа и марганца, Исслед. в области химии Всес. н.-и. и-та метрологии, **63** (1941). [12] Morrough, Metallurgia, **23**, No. 137, 151 (1941).

Comptes Rendus (Doklady) de l'Académie des Sciences de l'URSS
1943. Volume XXXIX, № 8

PHYSICAL CHEMISTRY

ON THE DIAGRAM OF CHEMICAL ACTIVITY OF GASES

By N. S. AKULOV, Member of the Academy of Sciences of the White Russian SSR

In a previous note [2] we have shown that by changing the pressure and temperature of the gas (or the volume and shape of the reaction vessel) one can obtain two principle states of chemically active gases: 1) Passive state, when under the given conditions no spontaneous initiation of the reaction is possible, i. e. in order to start it the conditions must be modified in at least a portion of the space filled with gas. 2) State of autogenesis, when after some lag τ (induction period) the reaction can arise spontaneously in the whole volume of the gas.

To either of these states there corresponds a certain region on the diagram p,T. The boundary between the regions is determined by the condition $\tau = \infty$ [1,2].

In the present note I shall show that two kinds of passive state can be obtained: 1) the state of reaction damping, or the «safety» state (I), when the reaction created in a portion of the space cannot spread to the adjoining regions, and is extinguished after some time; and 2) state of reaction spreading; or the combustible state (II), when the zone of reaction spreads from the initially created centre with a certain speed w*.

In its turn, the region of autogenesis falls, as will be shown later, into two regions: the region of spontaneous ignition, and the region of detonation (III and IV).

The calculation of the boundary between the passive region and that of autogenesis has been made in the preceding communication. For the calculation of the boundary between the safe and the combustible region, and for determining the speed of flame propagation, or, generally speaking, the reaction velocity, we shall first prove the following relation:

$$w = a\frac{L}{\tau} \qquad (1)$$

where L is the width of the flame zone, or the distance between the layer of gas, where the reaction comes to an end, and the layer, where it begins; and a is the coefficient of proportionality. In order to derive (1), we, first of all, should take into consideration that the time required for the flame front to move over a distance L is that, during which the reaction which has just started in a layer will come to an end, in other words, during an interval from the end of the induction period to the end of the reaction (reaction period τ_r). Yet, in virtue of the similarity rule, which requires that two kinetic curves could be brought into coincidence by changing the time scale, the reaction period τ_r is proportional to the induction period τ, and so we arrive at (1).

* By the heat evolved in the reaction zone the adjoining layers of the gas are continuously brought from the passive state to that of autogenesis, which accounts for the spreading of the reaction, of flame, in particular.

As for the dependence of the induction period upon pressure and temperature, it has been determined earlier. The only difference with the case here considered is that now τ in (1) should be taken not for the initial temperature of the gas T_0, but for certain mean effective temperature $T = T_0 + \Delta T$ which is established inside the moving flame zone of thickness L. If the reaction here were entirely adiabatic, the initial temperature T_0 would suffer an average increase of $\Delta T_a = \frac{Q}{C^*}$, where Q is heat of reaction, and C^*—specific heat of the gas. As a matter of fact; however, we should take $\Delta T = b\Delta T_a$, where b denotes the product of two proportionality coefficients, of which one is somewhat smaller than unity and characterizes a non-adiabatic process, and the other may greatly exceed unity and its presence is due to a departure from Maxwell's distribution in the run of the reaction. This departure consists in a relative increase of the number of active particles, i. e. of molecules with high energy, which in turn determine the run of the reaction. Thus, in formula (1) we should for τ put

$$T = T_0 + b\Delta T_a \tag{2}$$

where b, generally speaking, can be a function of both the initial temperature and pressure,

The width of the flame layer L is also a function of p and T. We can easily find it in first approximation. In fact, the principle element in the mechanism of flame propagation (or, generally speaking, of the propagation of reaction) is the diffusion of active centres from the zone of reaction to those layers of gas to which the reaction moves later. It will be obvious that the longer the free path of the molecule λ, the greater the depth to which under otherwise equal conditions the active centres should penetrate, and the wider the zone L. But the length of the free path varies inversely to the gas concentration, and accordingly, is proportional to $\frac{T}{p}$. Thus, we obtain

$$L = a' \frac{T}{p}, \tag{3}$$

where a' is a dimensionless coefficient, constant in first approximation. It may be remarked that if the free path is taken for unit of length, the constancy of the relation $\frac{L}{\lambda}$ is only a particular case of the invariance of expressions characterizing the state of a system, where the processes determined by the duffusion of molecules take place. Accordingly, the distribution of temperature within the flame zone is likewise invariant in first appoximation, if λ is taken for the unit of distance. Neither should the absolute increase of temperature ΔT_a inside the flame zone be dependent upon the concentration of gas if we neglect the loss of heat through the walls, because the increase of concentration is concomitant with the increase of specific heat and of the heat of reaction. Thus, inasmuch as the absolute increase of temperature and the distribution of temperature (in first approximation) are independent of either pressure or the initial temperature of gas, the mean temperature inside the flame zone also exceeds the initial temperature by a constant value not variable with either p or T. However, the increase of the effective temperature ΔT compared to the initial temperature T_0 does, generally speaking, depend upon p and T, because the departure from Maxwell's distribution depends upon the velocity of the reaction.

Hereafter we shall neglect this dependence, however, in first approximation, and shall therefore consider ΔT as a constant parameter, determined from the experiment. Now all data are in our possession for the calculation of both the boundaries of the combustible region and of the velocity of flame propagation at any point within this region. As for τ, we have already shown in our previous communication that we have the following expression for the time of retardation (for $E' = 0$):

$$\tau = \tau_0 \frac{\frac{1}{C_s^2} C_2 + C + \frac{1}{2C^2}}{\left[\left(1 + \frac{C^2}{C_s^2}\right) C_2 - \left(C + \frac{1}{2C^2}\right)\right] C}, \tag{4}$$

where

$$C_2 = \frac{3}{2} e^{\frac{E}{R}\left(\frac{1}{T_m} - \frac{1}{T}\right)} \tag{5}$$

is concentration, practically corresponding to the second limit in the middle portion of the self-inflammation peninsula *.

Remember that the parameters in (4) and (5) are defined by the two points $M(p_m, T_m)$ and $S(p_s, T_s)$, namely by the apical point of the peninsula and the apical point of the bay. C_m is taken for concentration unit. Thus, $C = \frac{pT_m}{p_m T}$. Substituting now (3) and (4) in (1), we find

$$w = w_0 \frac{\left(1 + \frac{C^2}{C_s^2}\right) C_2 - \left(C + \frac{1}{2C^2}\right)}{\frac{1}{C_s^2} C_2 + C + \frac{1}{2C^2}}, \tag{6}$$

where T should be put equal to $T_0 + \Delta T$.

Determining the equation of boundaries by means of (6) from the condition $w = 0$, we obtain

$$\left(1 + \frac{C^2}{C_s^2}\right) C_2 = C + \frac{1}{2C^2}. \tag{7}$$

Naturally enough, this equation is analogous to that defining the boundaries of the region of autogenesis. The latter is obtained from (4) and from the condition

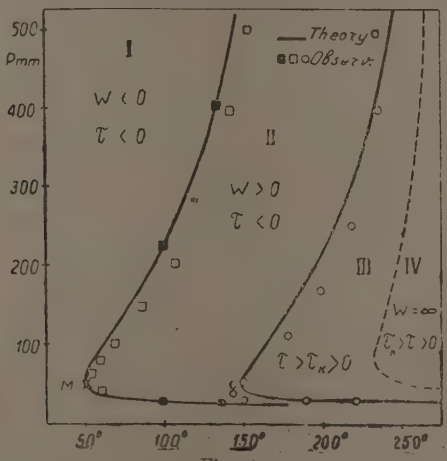

Fig. 1

$\tau = \infty$. In this case, however, we should put $T = T_0$ instead of $T = T_0 + \Delta T$. Thus, the extinction region has its boundary shifted to the left by as much as the value of ΔT with respect to the boundary of the autogenesis region.

Inside the peninsula of flame propagation the relations $\frac{C_2}{C_s^2}$ and $\frac{C^2}{C_s^2}$ may be neglected, and (6) can assume a very simple form. Then the condition $\frac{dw}{dC} = 0$ gives $(C)_{w\max} = 1$ as the value of concentration, for which the speed of propagation is

* The condition $\tau < 0$ means that no autogenetic reaction is possible (only a catalytic reaction can take place, particularly, on the walls of the vessel).

a maximum. In other words, inside the peninsula the maximum velocity of flame propagation is attained at a concentration at which the ignition temperature is a minimum. I have found upon analysing the experimental data of Voronkov and Semenov for the velocity of a cold flame propagation in a mixture of CS_2 and oxygen that this simple rule is really fulfilled within the experimental error.

Choosing for the boundary curve of the autogenic region the position of its two critical points (50 mm for 423°C, 950 mm for 525°), we find $C_s = 15$ and $E = 6800$*.

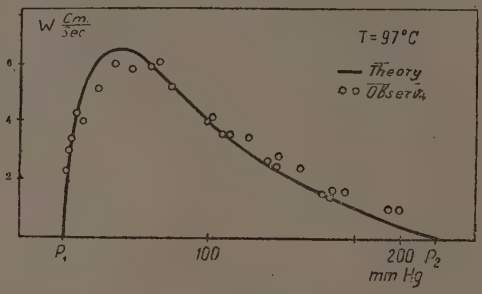

Fig. 2

Then equation (7) gives the boundary curve of autogenesis; which is compared with experimental data in Fig. 1. The boundaries of the safety region are determined by the displacement of this curve to the left by as much as ΔT. A corresponding

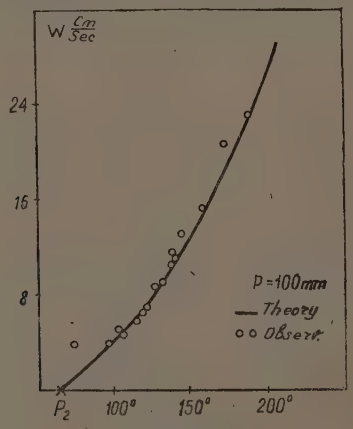

Fig. 3

curve is given for $\Delta T = 100$°C. The white squares indicate the results of direct observation of the moments when the flame propagation comes to an end. The black squares are the results of extrapolation of the velocity curve to $w = 0$. It may be seen that the theoretical curves reflect all the main peculiarities in the boundary run both for the region of autogenesis and for the extinction of safety region. Now we are able to calculate the velocity of flame propagation at any point of the combustible region (II). Let us take a vertical section at $T = 97$°C and a

* From (4) it follows with sufficient accuracy that $E\left(\frac{1}{T_m} - \frac{1}{T_s}\right) = R \ln \frac{1}{3} C_s$, where $C_s = \frac{p_s T_m}{p_m T_s}$.

horizontal section at $p = 100$ mm Hg. The respective theoretical curves are compared with experimental data in Figs. 2 and 3. In order to calculate these two curves we had only to use in addition a scale factor w_0 which we put at 5.2.

Thus, the developed theory which had arisen from the general relation of the new chemical dynamics, for the first time describes the totality of the fundamental experimental facts bearing on the properties of the combustible region and the region of autogenesis. The principle properties of the autogenesis region have already been considered quantitatively. In particular, we were able to calculate the thermal rate of reaction $\frac{da}{dt}$ and also the boundary outline of this region (where $\frac{da}{dt} = 0$). In the next communication entitled «On the thermal autoacceleration reactions» I intend to show that with gradual penetration inside the region of autogenesis the rate of reaction eventually reaches a certain critical value, whenever the reaction continues with steadily increasing thermoacceleration until it comes to an end. This exactly serves as the criterion of an explosion type of reaction. Thus, the region of autogenesis falls into two regions: the self-inflammation region (which in terms of the former theory might also be called the region of degenerated explosion; this term, however, fails to reflect the essential of the phenomenon) and the detonation region. In Fig. 1 the boundary between these regions (III and IV) is represented schematically.

Received
12. XII. 1942.

REFERENCES

[1] N. S. Akulov, C. R. Acad. Sci. URSS, XXXIX, No. 5 (1943). [2] N. S. Akulov, ibid., XXXIX, No. 6 (1943). [4] В. Г. Воронков и Н. Н. Семенов, ЖФХ, XIII, No. 12, 1695 (1939).

Comptes Rendus (Doklady) de l'Académie des Sciences de l'URSS
1943. Volume XXXIX, № 8

PHYSICAL CHEMISTRY

TWO TYPES OF *S*-CURVES IN ISOTHERMAL TRANSFORMATION OF SUPERCOOLED AUSTENITE

By N. N. SIROTA

(Communicated by N. P. Chizhevsky, Member of the Academy, 5. XII. 1942)

The transformation of supercooled austenite of carbon steels at subcritical temperatures is described by the well-known *S*-curve which Davenport and Bain (1) were the first to establish experimentally in 1930. Later investigations have revealed the existence of two types of *S*-curve. The first type is typical of carbon steels and of steels alloyed with non-carbidogenic elements. In these steels a region of accelerated transformation of supercooled austenite is observed at temperatures between the critical point A_1 and the martensite point M. Curves of the second type are characteristic of steels alloyed with carbidogenic elements (chromium, molybdenum, vanadium and tungsten). In this case there are two regions of accelerated transformation of supercooled austenite within the range of temperature above-mentioned.

The variation of stability in a supercooled austenite of carbon steels according to transformation temperature may, and so can also the shape of the *S*-curve, be readily interpreted in terms of the combined influence of the rate at which the centres of transformation arise, and of the linear rate at which they grow. This was first shown by Stark, Mirkin and Romansky (2).

But in the case of steels with special carbides the transformation of austenite and the shape of the respective *S*-curves require additional conditions in order to be adequately explained. Below we shall show qualitatively that the appearance of a second region of reduced stability of supercooled austenite is due to a change in the chemical composition of the products of its transformation, which is affected by the degree of supercooling. We shall deal here only with such *S*-curves as are plotted for the half-transformation time; since that period is the most convenient characteristic to indicate the stability of supercooled austenite upon isothermal transformation.

It is known (3) that the quantity of transformed austenite V_t toward the time t may for a perfectly three-dimensional growth of the transformation centres be expressed by the relation

$$V_t = 1 - e^{-w_3 k c^3 t^4}, \qquad (1)$$

where w_3 is the probability that the centres of transformation products will arise in a unit of untransformed volume in unit time; c is linear rate of growth of the arising centres; t, time elapsed since the outset of transformation; k, a constant dependent upon the shape of the growing centres.

From this, for the half-period of transformation t_{50}, during which 50% of the austenite is converted; we obtain

$$t_{50} = \sqrt[4]{\frac{k'}{w_3 c^3}}, \qquad (2)$$

where $k' = \frac{\ln 0.5}{k}$.

For expressing in an approximate manner the dependence of w_3 and c upon temperature, we make use of the relations similar to those set up by Volmer and Marder ([4]):

$$w_3 = \alpha e^{-\frac{A_3}{kT}}, \quad c = \beta e^{-\frac{Q}{kT}} e^{-\frac{A_2}{kT}}, \tag{3}$$

where A_3 is the work of separation of a three-dimensional nucleus of the new phase—the carbide; A_2 is the work of formation of a twodimensional nucleus of the new phase; k is Boltzman's constant; T, temperature; Q, activation energy of carbon atoms in the austenite; α and β are constants. The quantity $e^{-\frac{Q}{kT}}$ is proportional to the coefficient of diffusion of carbon in austenite.

The work of formation of two-dimensional and the work of formation of three-dimensional nuclei are interrelated, and in the simplest case of cubic nuclei either of them may be easily expressed by the other. The work of formation of a three-dimensional nucleus is expressed by the relation

$$A_3 = \frac{16\pi M^2 \sigma^3}{3\rho^2 R^2 T^2 \ln^2 \frac{c_r}{c_\infty}}. \tag{4}$$

For the work of formation of a two-dimensional nucleus the corresponding expression is

$$A_2 = \frac{\pi \varkappa^2 M}{\rho RT \delta \ln \frac{c_r}{c_\infty}}. \tag{5}$$

In these expressions M is molecular weight of the new phase; ρ, its density; c_r is concentration of carbon in austenite at the boundary with the separating carbide phase of radius r; c_∞ is equilibrium concentration at the boundary with the carbide phase formed of infinitely large dimensions; σ is surface energy of the formed phase at the boundary with the initial phase; $\varkappa$ is peripheral energy at the same boundary; δ, thickness of a two-dimensional nucleus.

For a cubic crystal, which is the simplest form, we have

$$\sigma = \frac{\varphi}{2r_0^2} \text{ and } \varkappa = \frac{\varphi}{2r_0},$$

where φ is the work expended in breaking one atomic bond; r_0 is distance between atoms. Whence

$$\varkappa = r_0 \sigma. \tag{6}$$

Since $\ln c = -\frac{3\varphi}{kT} + \frac{5}{2} \ln T + i$, where i is chemical constant, one may write in an approximate manner

$$\ln \frac{c_r}{c_\infty} = -\frac{3\varphi}{kT} \cdot \frac{\Delta T}{T_k}, \tag{7}$$

where ΔT is the degree of supercooling; T_k is critical temperature.

Making use of the relations (6) and (7) for expressing A_3 and A_2, we have

$$\left.\begin{aligned} A_2 &= k_2' \sigma \left(\frac{T_k}{\Delta T}\right) \\ A_3 &= k_3' \sigma \left(\frac{T_k}{\Delta T}\right)^2 \end{aligned}\right\}. \tag{8}$$

Then, by virtue of (2),

$$\ln t_{50} = \frac{1}{4} \ln k' - \frac{1}{4} \ln w_3 - \frac{3}{4} \ln c.$$

Substituting the values w_3 and c from (3) and (8), we obtain:

$$\lg t_{50} = K + \frac{k_1}{T} + k_2 \frac{\sigma}{T} \frac{T_k}{\Delta T} + k_3 \frac{\sigma}{T} \left(\frac{T}{\Delta T} \right)^2, \qquad (9)$$

where k_1 is a quantity dependent upon the coefficient of diffusion and K, k_2 and k_3 are constants.

From the obtained relation (9) it follows that for a given temperature the stability of the supercooled austenite increases with the surface energy σ of the separating phase, the carbide phase, for instance.

In the figure the relation (9) is represented graphically in coordinates. Absolute temperature is plotted against the logarithm of the half-transformation period for different values of σ ($\sigma_1 : \sigma_2 : \sigma_3 : \sigma_4 : \sigma_k = 1 : 1.2 : 1.4 : 1.6 : 2.0$).

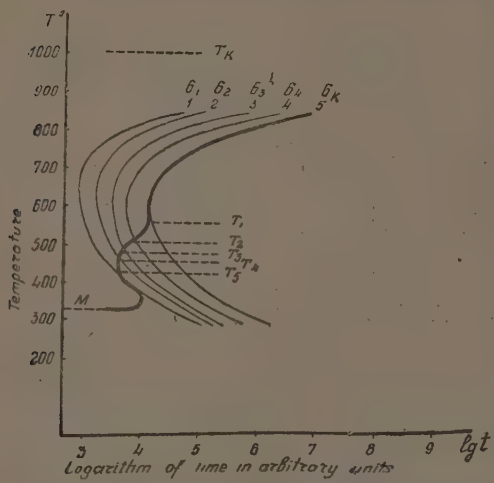

Half-transformation period of supercooled austenite in relation to temperature for different values of the surface energy of separating carbides.—Resultant curve of relation to temperature for t_{50} of alloy steel austenite, allowance being made for change in the composition of separating carbides within the interval T_1—T_5

In plotting the curves 1—5 the following values were adopted: $K = 0.5$; $k_1 = 2000$; $k_2 = 125$; $k_3 = 25$. From the plot it is seen that for constant values of σ the dependence of the stability of supercooled austenite on temperature, as obtained from equation (9), is represented by an S-curve similar in form to those obtained experimentally. In deriving equation (9) the composition of the developing phase and the mechanism of transformation are supposed to be liable to no variation in the transformation process at any temperature within the range considered.

As the surface energy of the separating carbide increases, so does the stability of the austenite, and the S-curve is shifted to the right.

In steels alloyed with carbidogenic elements the composition of carbides separating upon the transformation of supercooled austenite is variable with the degree of supercooling: as the latter grows, the composition becomes more simple approaching to the composition of iron carbide Fe_3C. This is a fact established experimentally and explained by us in the light of Ostwald's step rule [5]. In connexion with the change of the chemical composition of the separating carbides there is a change in the work expended in the formation of two- and of three-dimensional nuclei A_2 and A_3, this work approaching to that of formation of cementite nuclei. Here the stability curve is shifted to the left and comes near to that observed with the austenite of plain carbon steels.

In steels with alloyed carbides the stability curve of supercooled austenite shifts from the position corresponding to the separation of transformation products with a large value of σ towards the curves obtained for smaller values of σ. This accounts for the appearance of a second minimum of reduced stability of supercooled austenite in steels containing carbidogenic elements.

The appearance of the second type of S-curve can be interpreted on the basis of the graph shown in the figure. Upon the transformation of austenite in an alloy steel containing, when annealed, a carbide in equilibrium with the value σ_k, there is observed a separation of carbides within a temperature interval of T_k—T_1.

which are near to the equilibrium carbide in composition and have a surface energy approaching to the equilibrium value of σ_1. When the temperature ranges from T_1 to T_2, the separated carbides are lower in alloying elements than are equilibrium carbides, and have a surface energy of σ_4—σ_3. Within the temperature range of T_2—T_4 carbides with a surface energy of σ_3—σ_2 are separated, and when the range of temperature is T_4—T_5 the separated carbides have a surface energy of σ_2—σ_1 and approach to cementite in both their surface energy (σ_1) and composition. In the plot the temperature interval T_1—T_5 corresponds to T_1—T_2 represented in Fig. 1 of the above-cited article ([5]).

The resultant curve for the half-transformation period in the case considered is represented in the figure as a heavy line; it has two stability minima of supercooled austenite, and in its lower portion has shifted from position *5* to *1*; hence the appearance of a second minimum.

In different steels the composition of carbides may change to a different extent and at different temperature intervals. This accounts for the variety of individual forms among the *S*-curves of the second type. Since at low transformation temperatures the transformation products formed contain the least quantity of carbidogenic elements, it is obvious that the influence of the latter will be the stronger, the lower the degree of supercooling. In the case of strong supercooling they will approach in action to non-carbidogenic elements. The rôle of collateral factors has not been considered here, because they have no bearing on the deviation of *S*-curves into the two types above-mentioned.

Received
5. XII. 1942.

REFERENCES

[1] E. S. Davenport and E. C. Bain, Trans. AIME, **90**, 117 (1930). [2] Б. В. Старк, И. Л. Миркин, А. Н. Романский, Труды Моск. ин-та стали им. И. В. Сталина [3] N. N. Sirota, C. R. Acad. Sci. URSS, XXXVI, 192 (1942). [4] M. Volmer u. M. Marder, Z. Physik. Chemie (A), **154**, 97 (1931). [5] N. N. Sirota, C. R. Acad. Sci. URSS, XXXIX, 111 (1943).

Comptes Rendus (Doklady) de l'Académie des Sciences de l'URSS
1943. Volume XXXIX, № 8

GEOCHEMISTRY

HYDROCHEMICAL FACIES OF SURFACE GEOSPHERES

By G. A. MAXIMOVICH

(Communicated by W. I. Vernadsky, Member of the Academy, 29. I. 1943)

By a hydrochemical facies is meant the portion of aboveground and underground hydrosphere whose waters are throughout characterized by identical hydrochemical conditions as regards the predominance of certain dissolved substances (ions, colloids). The concentration and the chemical composition of the water in the particular portion are liable to certain variations, but the predominance of some definite substances is maintained.

A hydrochemical facies is determined by the first three (sometimes four or even more) components which exceed the other components in weight. The facies are given in the decreasing order of their significance. For different manifestations of the hydrosphere the following groups of hydrochemical facies or formations as defined by the predominance of a certain component have been established*.

Groups of hydrochemical facies or hydrochemical formations	Rivers	Lakes	Seas and oceans	Ground waters	Edge waters of the stratisphere
Silicious	+	+	—	+ ?	—
Hydrocarbonate	+	+	—	+	+
Calcium	+	—	—	+	—
Sulphate	+	+	—	+	+
Sodium	—	+	—	+	+
Chloride	+	+	+	+	+

Further investigation is likely to establish the silicious formation for the stratisphere also. The ground waters referring to this formation should, according to the analyses of fluvial waters; occur in the tropical zone and in the tundra.

Thus; with the exception of seas and oceans, the silicious; hydrocarbonate, sulphate and chloride hydrochemical formations are found in most of the water shells. The calcium hydrochemical formation, which is one of a poor stability, is known in the surface and underground streams. The sodium hydrochemical formation characterizes the rather immobile lake; ground and edge waters.

The bulk of sea and ocean waters; with the exception of small strips in the littoral waters, shows a concentration varying within fairly narrow limits; and these waters belong not merely to a single formation; but also to one facies (chloride-sodium-sulphate).

* It will be hardly correct not to take in account at water classification the organic substances sharply different in the tropic and the arctic belts.

In general little variation is also shown by hydrochemical facies of rivers and lakes, or by ground and edge subterranean waters. This in spite of the fact that every such manifestation of the hydrosphere is distinguishable by some specific facies. Therefore it is the composition of the gases as indicated by W. I. Vernadsky ([2], [3]), that should be considered as the main distinguishing feature of the hydrochemical facies of the different hydrospheres, their portions and manifestations.

The next problem is to characterize the gaseous composition of different hydrochemical facies, as well as of subsidiary mineral components in solution, and of the organic matter dissolved. In particular, oil-field waters are characterized by the presence of naphthenic acids ([7]). Enrichment with iodine and bromine ([4], [6]) is, along with helium-argon coefficient ([9]), a remarkable feature of pelogenic chloride-sodium-calcium waters of the stratisphere, destitute of sulphate.

The hydrochemical facies of rivers, lakes and ground waters displays zonal distribution. There are 5 main zones; the tropical zone, two steppe and desert zones, and two zones of moderate climate. Moreover, four subzones may be distinguished which; with increasing accumulation of hydrochemical data, are likely to rise to the rank of zones. These are two steppe subzones (one in the northern, the other in the southern hemisphere) and two zones of tundra. Apart from this, the rivers and lakes have also a vertical (mountainous) zone. Ground waters are scarcely developed in mountainous regions: they occur in the alluvium of river terraces, etc. and so they show no zonal distribution along the vertical.

Azonal phenomena may be caused by hydrological, geological and lithological peculiarities, and also by the activity of man.

Rivers and ground streams may several times change their facies along the direction of the flow. The majority of long rivers are polyfacial. Ground streams that cover a smaller range show a less facial change along their path. Lakes and ground basins change their hydrochemical facies not only in the horizontal, but also in the vertical direction. The gaseous composition of the lakes also varies along the vertical.

The hydrochemical facies of rivers, lakes and ground waters vary not merely in space, but also according to the age.

As a typical complex of predominant soluble substances in river, lake and ground waters, the hydrochemical facies indicates definite climatic conditions under which the concentration and formation of the composition of these waters went on; as well as soil, geochemical (weathering), hydrological and hydrogeological factors which are all correlated with the climate. A change of climatic conditions results in a change of hydrochemical facies and in the shifting of their zonal boundaries.

In the case of edge waters of the stratisphere the hydrochemical facies change with the distance from the outcrop of the stratum to the surface; which goes parallel with the increase in concentration. The activity of microorganisms is another important factor in the transformation of edge waters. The edge waters of the stratisphere, unlike fluvial, lake and ground waters, can be of syngenetic, as well as of epigenetic nature. The former are distinguishable by a peculiar hydrochemical aspect.

The hydrochemical facies vary not only along the strata, but in a series of strata they also vary along the vertical.

The character of hydrochemical facies of edge waters of the stratisphere is determined by the origin of the waters, by their concentration, by the composition of the reservoir and its inclosing rocks, and is also dependent on permeability, on the presence or absence of tectonic fissures and erosion phenomena that cause the denudation of the stratum, on the accumulation of organic matter, on the activity of organisms, on geotectonic and geomorphological conditions and, finally, is variable with the time elapsed since the waters were formed in the stratum (age).

The first in importance are the geotectonic and geomorphological conditions and also the permeability. Flat areas with a slightly dissected relief are characte-

rized by gases of biochemical and partly of atmospheric origin (1). They also contain strongly concentrated waters of chloride type (10). In the majority of cases, concentration grows with depth.

Geoanticlinal regions represented by modern mountainous folded structures are characterized by the presence of metamorphic gases in their centre. Away from the centre to the periphery the origin of the gases varies in the order: mixed metamorphic and atmospheric: atmospheric; atmospheric mixed with biochemical; biochemical. Generally speaking, the hydrochemical facies vary in the same direction, and the hydrocarbonate type is superceded by the sulphate, sodium and chloride type. However, denudation differences in the case of fissures and erosion, as well as the different perviousness account in many cases for the absence of a regular change of concentration or of hydrochemical facies along the vertical. This along with different composition of the rock gives rise to peculiar azonal phenomena which stand out in the otherwise zonal succession of hydrochemical facies depending upon the structure—from the centre of the mountainous folded region towards the platform.

Hydrochemical facies of edge waters of the stratisphere vary not only in space, but also with time. Changes in the rate of migration, feeding conditions bring about changes in the concentration and sequence of hydrochemical facies. The activity of man plays an important and gradually increasing part in the varying rate of migration of edge waters.

Among the facies of the surface hydrospheres; the hydrochemical facies of fluvial, lacustrine, ground and edge waters are the most labile. Thus, we are to add to the facies of the crust of weathering and the stratisphere (8), to the facies of the pedosphere (and various types of soils should practically be considered as such), to the facies of sedimentary, erruptive and metamorphic rocks [as well as to the biochemical provinces determined by A. P. Vinogradov(5)] also the highly mobile and variable hydrochemical facies.

Department of Dynamic Geology.
Molotov State University.

Received
29. I. 1943.

REFERENCES

[1] В. В. Белоусов, Очерки геохимии природных газов (1937). [2] В. И. Вернадский, Соц. реконструкция и наука, 2, 52 (1937); Первый Всесоюзн. гидрол. съезд, сб. 8, 65 (1933). [3] В. И. Вернадский, История минералов земной коры. II. История природных вод. ч. 1, в. 1 (1933); в. II (1934); в. III (1936). [4] A. P. Vinogradov, C. R. Acad. Sci. URSS, I. No. 4 (1934). [5] A. P. Vinogradov, ibid., XVIII. No. 4—5 (1938). [6] А. П. Виноградов, Тр. Биогеох. лаб., V, 29 (1939). [7] Классификация подземных вод нефтяных месторождений Апшеронского полуострова (1934). [8] Л. В. Пустовалов, Пробл. сов. геол., 1, 57 (1933). [9] В. И. Савченко, Природные газы, сб. 8, 53 (1935). [10] Н. И. Толстихин, Пробл. сов. геол., 3, 240 (1938).

Comptes Rendus (Doklady) de l'Académie des Sciences de l'URSS
1943. Volume XXXIX, № 8

GEOLOGY

LOWER JURASSIC CHAIN OF VOLCANOES IN THE CENTRAL CAUCASUS

By L. A. VARDANIANZ

(Communicated by W. A. Obruchev, Member of the Academy, 30. VII. 1942)

Within the area of the Central Caucasus there have long been known manifestations of volcanism, for which a Lower Jurassic age has partly been proved and partly is highly probable. The origin of such rocks and their full geological petrographic characteristic were not established precisely until 1940 and they were described in literature by very indefinite terms, such as porphyries, ceratophyries, diabases, etc.

In 1940 one of the regions where such volcanic manifestations are developed, viz. the neighbourhoods of Mikoian-Shakhar in Karachay, were explored in detail by the present author on behalf of the All-Union Geological Institute. This investigation and the comparison of the results obtained with the materials on other parts of the Central Caucasus gave a clear-cut picture of the character and the scale of volcanic activity during the Lower Jurassic within an area comprising nearly all of the main range of the Caucasus.

At present it may be positively ascerted that at the time of the Lower Jurassic at least five separate volcanic regions existed in the Central Caucasus. Each of them was stretching along the range over a span of 50—100 km and included several volcanic centres acting simultaneously or in alternation.

Extreme towards the north-west was the region occupying the portion of the range between Tuapse and Sochi. Here the manifestations of volcanism were first established by K. I. Bogdanovich (1907) who identified them with mica dacites. Later works by O. O. Vialov (1931, 1934) and V. V. Beloussov (1937, 1939) have shown that in this portion of the range a series containing large amounts of eruptive rocks of the quartz-porphyry type and their tuffs is developed. The age of this series may probably be described as Toarcian; it is overlain by deposits which are very likely to belong to the Aalanian age. From thin-section of these rocks taken from the collection of O. O. Vialov, it may be inferred that typical liparites are here widely represented along with dacites. In this region (mount Chugush, for instance) andesites are also found (L. A. Vardanianz, 1938; G. M. Efremov, 1936, 1941), but they do not appear to play an essential rôle.

The second region comprises Karachaj and the upper reaches of riv. Podkumka on the northern slope of the range. Here volcanic formations are associated with a carboniferous series whose age is not older than the Pliensbach, not younger than the Toarcian (G. E. Pituchenko, 1940, and oth.). From faunistic evidence the Aalanian deposits are overlying the Carboniferous series uncomformably and transgressively (G. P. Agalin, 1929). In that region the Lower Jurassic was followed only by disjunctive tectonics, and even this is expressed comparatively weakly.

Therefore intrusive as well as effusive and eruptive phases of volcanic activity can be established here with remarkable clearness. One may also distinguish there

alternation with relatively quiet periods, and also variations in the composition of the lava, the superposition of younger formations upon more ancient, the feeding apparatus of the volcanoes and even the relics of the Lower Jurassic. Very well represented are certain laccoliths completely opened by erosion from the roof to the underlying sedimentary rocks (L. A. Vardanianz, 1940).

With regard to mineralogical composition and structure, the lavas of this region range through a whole series of rocks from olivine basalts through pyroxene andesites to hornblende-biotite andesites and biotite dacites. Liparito-dacites, too, may be supposed to occur here. In some cases these rocks are so typical and fresh as to be absolutely undistinguishable from the classical neointrusions of the Central Caucasus. In the districts of Karachay the eruptions were followed by an intensive manifestation of post-volcanic processes which produced barite and quartz-carbonate aragonate veins, and occasionally the eruptive rocks were modified very considerably (L. A. Vardanianz, 1940). Similarly modified varieties have been described as ceratophyries (P. I. Lebedev, 1930).

The studies of 1940 have shown that the main lavas of this region are concentrated at the final stages of volcanic activity. At some places, however, e. g. near vil. Nizhne-Marinskoye, eruptions of dacite and basalt have taken place almost simultaneously and only 3 to 5 km apart from each other.

The third region comprises the Hulama gorge along riv. Cherek-Bezenghievsky and the adjoining parts of the neighbouring gorges. Here the volcanic formations are associated with a sand-shaly series of the Lower or Middle Lias overlain uncomformably by Aalanian deposits (I. G. Kuznetzov, 1940) and fall into two groups (D. S. Beliankin, 1915; I. G. Kuznetzov, 1940). One of them, that which appears to be more ancient, is represented by rocks coming near to trachiliparites, and the other, by rocks of the bazalt and andesite type. The first have so far been described as ceratophyries; the second, as diabases and porphyries.

The fourth region extends over Digoria, Ossetia and a portion of Ingushetia. Here there are two groups of volcanic formations, one of which is known by the name of ceratophyries and the other by the name of the diabases. The investigations by several different authors (L. A. Vardanianz, 1925, 1926, 1935; M. I. Izikson, 1940, and oth.) have shown that the ceratophyries compose a particular horizon which has been traced along a distance of nearly 100 km from the Shtulu path down to Dariel. Its age is now referred to the Lower and Middle Lias. It is overlain uncomformably by rocks including Toarcian fauna (M. I. Izikson, 1940). The ceratophyric horizon is mainly composed by tuffogenic formations; the predominant rocks here are andesites and dacites, very strongly albitized, chloritized etc. (L. A. Vardanianz, 1935). The centres of these eruptions have not yet been located iwth sufficient accuracy.

The second group of rocks in this region is represented by a full set, at one end of which are variolites and vitrophyres and on the other, diabases and gabbro-diabases (L. A. Vardanianz, 1937). The intermediate position is held by augite porphyries. This complex of rocks corresponds precisely to the diabasic formation of Chaokhi and Roshki in Ingushetia (T. I. Lewinson-Lessing, 1896). The presence of agglomerate lavas, variolites and tuffogenic rocks is evidence that this complex is synchronous to the enclosing sedimentary rocks which are mainly compact shales. This series was formerly referred to the Middle Lias (L. A. Vardanianz, 1935), but from more recent evidence (M. I. Izikson, 1940) appears to belong to Toarcian. At any rate the diabase-variolate complex is younger than the ceratophyric complex, and for it three main centres of erruption may be suggested: Fiagdon, Genaldon-Kazbeck, and Chaokhi-Roshki (L. A. Vardanianz, 1937).

To sum up, a transition from more acid lavas, emitted during the first phases of eruption, to more basic ones of the subsequent phases can be clearly traced in the Digoro-Ossetian district.

The fifth region lies in North Kakhetia and has many features in common with that of Digoro-Ossetia. Here albitophyric (ceratophyric) tuffs of a rather considerable thickness, on the one hand, and diabases, vitrophyres etc. with their attending tuffs, on the other, are associated with the sand-shaly formations of the Lower

and Middle Lias. Just as in Digoro-Ossetia; the albitophyres are the most ancient formations; and underlie the sand-shaly series; in which diabases and other rocks are included in the form of dykes and strata (L. A. Vardanianz; 1932; 1940). The presence of tuffy formations again points unmistakably to a generally synchronous origin of diabases and their enclosing shales. More precisely; the age of ceratophyries and diabases of Kakhetia has not yet been established; but there is no doubt that it is younger than the Toarcian.

Thus, in the interval between the upper portions of the Lower Lias and the lower portions of the Upper Lias; the zone of what to-day is the Caucasus range presented a chain of volcanoes very similar to that which had existed here during the Pliocene and post-Pliocene. The latter is known to have been composed by at least four regions: Elbruz, with the predominance of dacite and andesite lavas; Cheghem; in which liparites were extensively developed; Digora; where the main rôle was played by dacites and andesites; and the Kazbeck region; in which andesites predominated. The similarity is emphasized not merely by the set of lavas; but also by the circumstance that the maxima of activity failed to coincide in different regions. Thus; in the Cheghem region the maximum of activity falls within the Upper Pliocene; in the Kazbeck region; whithin the post-Pliocene; and the Elbruz region appears to have been active both during the Pliocene and post-Pliocene. In the Lias chain of volcanoes; too; the maxima of activity show no complete coincidence in different regions. The similarity extends to the fact that both in the ancient and in the young chain of volcanoes each volcanic region included several centres of eruption; and these centres; though acting simultaneously and being situated very close to each other; did not all eject the same kind of lava; while the lava of some was acid; others emitted a basic lava.

The formation of Middle Lias volcanic chain within the area of the Central Caucasus was intimately related with orogenic. movements that occurred between the Rhaetic and Aalanian. Towards the outset of Aalanian transgression the volcanic activity here was stopped for long, at least in the effusive form. A similarly close connexion with orogenic movements is observed in the Upper Pliocene chain of volcanoes of the Central Caucasus.

All-Union Geological Institute.
The North Caucasus Geologic Administration.

Received
30. VII. 1942.

Prix $ 0.50